Development of a Textile Integrated, Two-State Controlled Tremor Suppression Orthosis for the Wrist

Nicolas P. Fromme, Adrian Esser, Martin Camenzind, Veit Mylius, Christian Baumann, Fabian Büchele, Robert Riener, *Senior Member, IEEE*, Peter Wolf, and René M. Rossi

***Abstract*—Tremor is one of the most common movement disorders with the highest prevalence in the upper limb. Apart from medication or surgery, the mechanical suppression of the involuntary movement with an orthosis can be used as alternative treatment. Here we propose a controlled energy dissipating suppression orthosis using a mechanical brake. For this approach, we focused on improved wearability with voluntary movement preservation and ergonomics while providing tremor suppression. The novelty of this orthosis is the decentralization of the tremor suppression mechanism and the integration of textiles in the orthosis structure. We performed computational and test bench simulations of a controlled two-state brake with a 1D human model to optimize the brake duration and timing. The objective was to optimize the trade-off between tremor suppression and voluntary movement suppression. The textile-integrated prototype, with the optimized parameter, was validated in a proof-of-concept case study with a tremor-affected person performing activities of daily living. With the optimized parameters, we achieved a tremor suppression of 78.8%, 66.5%, and 40.8% for the simulation, test bench, and case study, respectively as measured by the change in power spectral density (PSD) at the tremor frequency peak. While minimizing the voluntary movement suppression in the simulation and test bench by introducing the trajectory distance as new validation method (23.7% and 31.2%), no voluntary movements suppression was measured in the case study using PSD analysis. Our new orthosis has the potential to become a daily wearable device that can improve the quality of life for tremor-affected people.**

***Index Terms*—Exoskeleton, soft robotic suits, tremor, suppression.**

Manuscript received 25 May 2022; revised 1 September 2022 and 19 December 2022; accepted 13 March 2023. Date of publication 7 July 2023; date of current version 9 August 2023. This article was recommended for publication by Associate Editor J. Patton and Editor P. Dario upon evaluation of the reviewers' comments. *(Corresponding author: Martin Camenzind.)*

This work involved human subjects or animals in its research. Approval of all ethical and experimental procedures and protocols was granted by the Ethics Committee of Eastern Switzerland (EKOS).

Nicolas P. Fromme is with the Empa, Laboratory for Biomimetic Membranes and Textiles, Swiss Federal Laboratories for Materials Science and Technology, 9014 St. Gallen, Switzerland, and also with the Sensory-Motor Systems Lab, Department of Health Sciences and Technology, Institute of Robotics and Intelligent Systems, ETH Zurich, 8092 Zürich, Switzerland (e-mail: Nicolas.Fromme@outlook.com).

Adrian Esser and Peter Wolf are with the Sensory-Motor Systems Lab, Department of Health Sciences and Technology, Institute of Robotics and Intelligent Systems, ETH Zurich, 8092 Zürich, Switzerland (e-mail: Adrian.Esser@hest.ethz.ch; Peter.Wolf@hest.ethz.ch).

Martin Camenzind and René M. Rossi are with the Empa, Laboratory for Biomimetic Membranes and Textiles, Swiss Federal Laboratories for Materials Science and Technology, 9014 St. Gallen, Switzerland (e-mail: Martin.Camenzind@empa.ch; Rene.Rossi@empa.ch).

Veit Mylius is with the Department of Neurology, Center for Neurorehabilitation, 7317 Valens, Switzerland, and also with the Department of Neurology, Philipps University, 35037 Marburg, Germany (e-mail: Mylius@med.uni-marburg.de).

Christian Baumann and Fabian Büchele are with Department of Neurology, University Hospital Zurich, 8091 Zürich, Switzerland, and also with the University of Zurich, 8092 Zürich, Switzerland (e-mail: Christian.Baumann@usz.ch; Fabian.Buechele@usz.ch).

Robert Riener is with the Sensory-Motor Systems Lab, Department of Health Sciences and Technology, Institute of Robotics and Intelligent Systems, ETH Zurich, 8092 Zürich, Switzerland, also with the Medical Faculty, University Hospital Balgrist, 8008 Zürich, Switzerland, and also with the University of Zurich, 8092 Zürich, Switzerland (e-mail: Robert.Riener@hest.ethz.ch).

Digital Object Identifier 10.1109/TMRB.2023.3293192

I. Introduction

TREMOR is defined as the rhythmic and involuntary oscillatory movement of a body part [1]. It is one of the most common movement disorders in adults [2]. Among many, Essential Tremor (ET) and Parkinson Disease (PD) are the two most common conditions causing tremor, and the hand is the most affected body part [3], [4], [5], [6]. ET is observed in 4.6% of the population aged over 65 and in 21% over 95, while PD is observed in 2% over 65 [7], [8]. ET incidences increase with age, whereas young people can also be affected [9], [10]. Tremor can be distinguished between action and rest tremor where rest tremor appears in the affected body part when it is not voluntarily activated, and action tremor occurs with the voluntary activity of the limb [11]. Tremor, especially action tremor, disturbs activities of daily living. More than 65% of the population with upper limb tremor have difficulties in activities of daily living, including many working tasks [6], [12].

ET and PD cannot be cured, so treatments focus on relieving the symptoms and increasing the quality of life for patients [13]. Medication is the most common treatment, with reduced efficacy of 23% to 59% for PD [14] and 39% to 68% for ET patients [3]. However, 53% of patients will discontinue medical interventions due to side effects or lack of efficacy [14], [15]. Deep brain stimulation (DBS) is the most effective treatment but is reserved for advanced cases due to its risk [3], [15], [16]. Up to 48% of patients undergoing surgery for DBS faced adverse events [15], [16], [17].

Even with optimal medical or surgical intervention in tremor patients still require physical and occupational therapy interventions to promote full social participation [18].

TABLE I
SUMMARY OF OBJECTIVES AND HYPOTHESES

		Objective/Hypothesis
O1	O1.1	Finding optimal values for the controller parameters, brake duration and delay time, through simulation.
	O1.2	Validating the optimal values for the controller parameters, brake duration and delay time, with a test bench.
O2		Evaluate the orthosis prototype with an optimized controller in a single human trial.
H1		The orthosis prototype suppresses tremor in the magnitude of devices in literature (30%-98) while preserving voluntary movements.
H2		The perceived wearability and voluntary movement preservation of the orthosis are good by being in the upper third of the rating scale of the custom questionnaire.
H3		The human trial study verifies and confirms the simulation and test bench outcome regarding the impact of the control parameter on the tremor suppression efficacy.

For example, people who are refractory to medication, which applies to 50% of ET patients, need additional treatments such as functional electrical stimulation, limb cooling, vibration and more recently peripheral electrical stimulation of afferent (sensory) pathways [15], [19], [20], [21]. Peripheral electrical stimulation is getting high scientific and clinical interest as no surgical intervention is needed, wearable devices are available and the method has a reported efficacy of 40% to over 80% [19], [22]. Another promising approach is the external treatment of tremor by physically suppression with the limb by either modifying the joint impedance or introducing an external force.

Tremor suppression orthoses have been developed for physical interaction with the (affected) limb. Such orthoses can be classified by the type of tremor suppression mechanism employed: active as force inducing, passive as energy dissipation and/or absorption, and semi-active as actively controlled energy dissipation and/or absorption [23]. Active systems can offer tremor suppression efficacies in the range of medication, but the high weights at the distal portion of the limb and interference with voluntary movements lead to bad wearability and poor acceptance by the wearers [24], [25]. Passive mechanisms modify the human joint impedance by increasing the damping, inertia and stiffness, which results in tremor suppression [26], [27]. However, an increase in impedance also decreases voluntary movements [28]. The active control of impedance with semi-active mechanisms allows tuning the impedance according to the tremor frequency and individual needs. Such an active control gives the possibility to follow voluntary movements without the need for an actuator and the accompanying high weight. Semi-active devices rely on energy absorption mechanisms, such as pneumatic cuffs [29]. Such systems can alternatively or additionally rely on energy dissipation mechanisms, such as magnetic tuneable viscous shear resistance (e.g., magneto-rheological fluids [27], [30], [31], [32], [33], [34], [35]), or friction damping, such as electromagnetic brakes [36].

The electromagnetic suppression mechanisms proposed by Herrnstadt and Menon were developed for the elbow and reported to have suppressed over 88% of tremor power (healthy participants) [36]. The proposed suppression mechanism is promising, but as it is bulky and rigid and weighs 942g, wearability for everyday use is limited [37]. Semi-active systems present the opportunity of combining the advantages of passive system with its light weight and active systems with the voluntary movement preservation.

Therefore, we propose a new approach with special emphasis on the wearability to implement an electromagnetic brake with a controller into a tremor suppression orthosis. To overcome many of the shortcomings, we propose a decentralized electromagnetic brake that is placed at the forearm and is coupled to the wrist via a rope. The brake can change between two states where OFF implies no impedance change and ON high impedance change (friction damping), switchable within milliseconds. A two-state (ON/OFF) braking system was used as the system actuator primarily for its simplicity, light weight, and compactness. Such factors are integral for the development and eventual adoption of soft wearable technologies in and outside of the research environment, and should be considered in the design process [38]. As tremor is most concentrated (highest peaks at a stereotyped frequency) in wrist flexion-extension for action tremor such as ET, the device was designed for this degree of freedom [39]. In Parkinson's Disease also pron-supination is predominant.

The brake, in combination with the active control, offers the possibility to adapt the impedance in the millisecond range. With this hardware, a mechanical notch-filter can be designed, filtering only tremorous frequencies (ranging from 3Hz to 12Hz [4]) and preserving the frequency of voluntary movements (ranging from 0Hz to 2Hz [40]).

To provide wearability and thus acceptance, the orthosis was incorporated into textiles. Textiles are a favourable material for wearable devices as they present flexibility, adaptability, low weight, breathability, washability and soft hand-feel [41]. We present for the first time a tremor suppression orthosis using textiles as well as a decentralized suppression mechanism.

Our first objective (O1) was to identify control parameters, brake duration and timing (delay time) of the brake that maximally suppress tremor while minimally suppressing voluntary movements (see Table I). Therefore, we first optimized the control parameters through computer simulation and determined the tremor suppression efficacy and voluntary movement preservation as well as the influence on the human joint system dynamics (O1.1). Additionally, we verified the validity of the model on a test bench (O1.2).

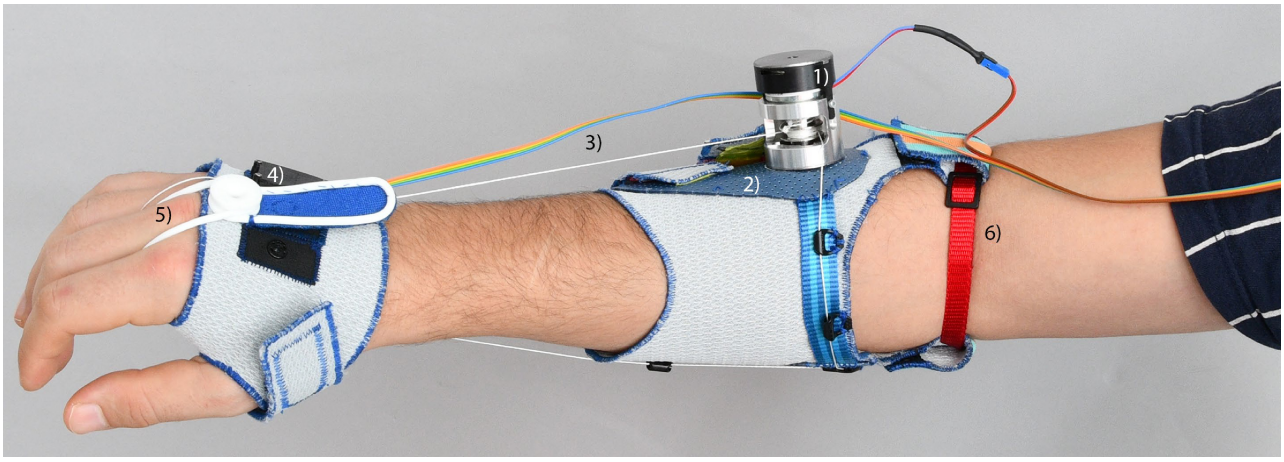

Fig. 1. Demonstrator of textile, semi-active orthosis, with the brake 1) connected to the thermoplastic plate 2), the rope 3), and gyroscope 4). The straps 5) and 6) are force anchoring points to the human.

The second objective (O2) was to evaluate the orthosis prototype with the optimized controller in a case study. For this objective, three hypotheses were proposed. First, we expected that the proposed semi-active tremor suppression orthosis would suppress tremor in the magnitude of 30% to 98% while preserving all voluntary movements during different activities of daily living. These values match the ranges of tremor suppression seen in devices in the literature (hypothesis H1) [37]. Second, we expected that the perceived wearability and voluntary movement preservation of the orthosis would be rated in the upper third of the custom questionnaire, indicating acceptance of the device by the user (hypothesis H2).

Finally, we expected that the human trial study would demonstrate the effectiveness of the optimal control parameters for tremor suppression (hypothesis H3). It is also expected to see a decrease in the efficacy of the system during subject testing compared to the tests in simulation and on the test bench.

II. Methods

A. System Hardware Design

A textile-integrated orthosis was designed to improve wearability for the wearer. The orthosis coupled the extension and the flexion of the wrist with a rope (see Fig. 1). The rope was anchored at the palmar and dorsal side of the hand. The rope was deflected about 90° on the dorsal side of the forearm to the volar side, where it was again deflected about 90° back to the palm, creating a closed motion coupled loop. When extending the wrist, the rope is pulled at the palmar side and shifted from the dorsal side around the two deflection points to the volar side and vice versa when flexing the wrist. At the deflection point on the dorsal forearm side, a brake was integrated. When activating the brake, the rope was held in place, preventing its movement and thus of the hand.

The ON/OFF brake, an electromagnetic clutch (6W, 24V) that generates a torque of up to 0.2Nm within 13ms by friction (86 011.03.E00, Kendrion N.V., Amsterdam, The Netherlands), was connected to a shaft onto which the rope was spooled. The spooling shaft of the brake, with a diameter of 12mm, was separated into two compartments, one for the dorsal rope side and one for the volar side [42]. This design avoided an overlapping and therewith prevented a blocking of the upwinding and unwinding rope. Even though mostly textiles were used, the brake unit was screwed onto a 1.6mm breathable (perforated) thermoplastic sheet (1.6mm Rolyan Splinting Sheet, 13% UltraPerf Perforated, Performance Health International Ltd., Sutton-in-Ashfield, U.K.), which was slightly bent to fit the forearms shape. Another piece of the thermoplastic sheet (ca. 30mm diameter) was used to anchor the second 90° rope deflection point on the palmar side of the forearm. To ensure minimal friction at the deflection point, a BOA lace guide was implemented. The thermoplastics sheets were sewed from hand onto the textile. As rope, a 0.4mm ultra-high-molecular-weight cord braided from polyethylene spun fibres (Dyneema 50daN, Koninklijke DSM N.V., Heerlen, The Netherlands) was used. Its low stretch of <1% and low friction coefficient were desired for this application [43]. When the brake was on, the stretch of the rope acted as a spring by absorbing and delaying force transmission, and when the brake was off, the friction of the rope on the guide and in the brake acted as a damper creating a resistive force. The rope was clamped on the dorsal and palmar side of the hand using snap buttons. The reactive forces of the brake mechanisms were anchored at the elbow using a strap, which was based on orthopaedic technology measures. A similar force anchoring method is used in prostheses [44]. In previous tests on healthy subjects, design adaptations and parameter tuning were done to ensure no restrictions in the range of movement before performing tests with patience. Additionally, for increased force connection of the textile orthosis to the wearers' limb, the textile was partially coated with silicon (Alpatec 30203, CHT Switzerland AG, Montlingen, Switzerland). The silicon coating improved the transmission of shear forces onto the skin, preventing chafing and shifting of the orthosis. The total weight of the orthosis was 152g, not considering the power supply and controller.

A gyroscope sensor (FSM305, Hillcrest Laboratories, MD, USA) running at 200Hz was placed on the dorsal side of the hand, anchored and protected in a custom 3D printed housing. Sensor data acquisition and brake controls were implemented

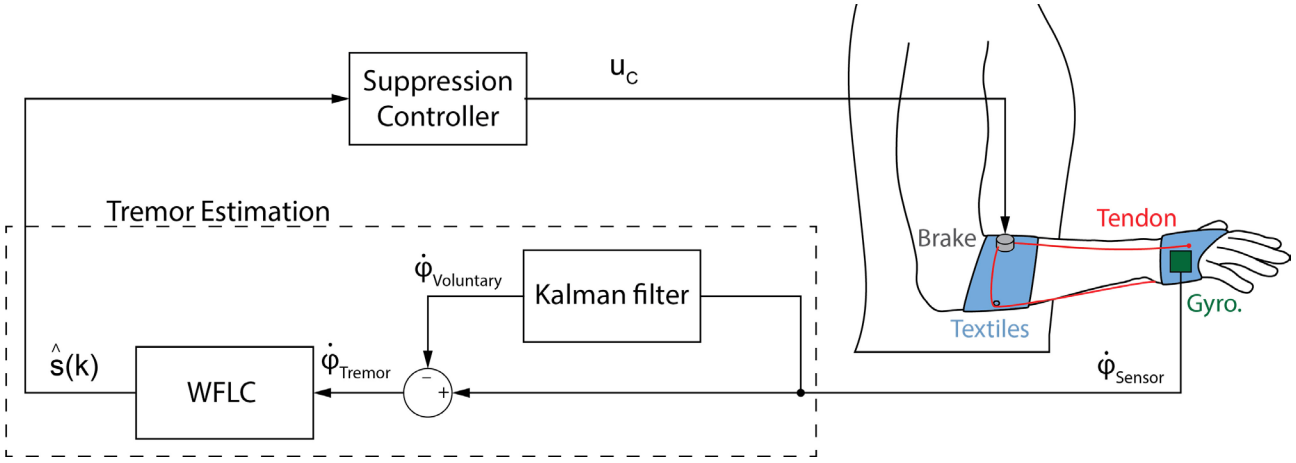

Fig. 2. Control scheme of the orthosis. The Kalman filter combined with the WFLC provided a dynamic tremor estimation model ŝ(k) based on the angular velocity $\dot{\varphi}_{sensor}$ measured from the gyroscope sensor on the hand. The suppression controller triggered the step signal based on the zero-crossing of the predicted tremor estimation model and delayed the onset based on the adjustable tremor delay time parameter. This controller adjusted the length of the brake voltage step signal u_c based on the brake duration parameter.

on a 32-bit microcontroller (Teensy 4.0, PJRC.COM, LLC, OR, USA) running at 600MHz.

B. Control Strategy for Tremor Suppression

A mechanical notch filter should be realized by the brake to mechanically filter the tremor-dominated frequencies, creating a counteracting force to the tremor. The brake control was designed to brake periodically for an optimized duration and at an optimal time in the sinusoidal tremor cycle (delay time). The optimized parameter were determined by identifying the highest tremor suppression paired with the lowest voluntary movement suppression. Determining the optimal brake duration and timing was one objective in this study (O1).

1) Tremor Model: A tremor model was required to compensate for the latency of the brake so that the brake could be activated at any desired delay time. From the time when the signal to the brake was given until the brake closed fully, 13ms passed [45]. With a simple sensory-based threshold-crossing control, like the one used by Kalaiarasi and Kumar [29], the optimal offset in the tremor cycle might be missed. Furthermore, a tremor model is important to analyze the tremor frequency to assess and account for its frequency shift, which is considered important to counteract tremor [46]. Tremor signals are non-stationary with variable frequency; thus their analysis cannot be carried out using the conventional Fourier transformation. Applying a discrete Fourier transformation to the signal reveals its spectrum of frequency content. However, this spectrum does not show the time dependency of the signal [47]. The control system required to dynamically model the tremor velocity in real-time is based on the received gyroscopic data. Here, we implemented a Weighted-frequency Fourier Linear Combiner (WFLC) developed by Riviere for the adaptive suppression of tremor for improved human-machine control in surgery (see Fig. 2) [48]. The WFLC is an adaptive algorithm that builds a tremor estimating, sinusoidal model by estimating its time-varying frequency, amplitude and phase. Although other algorithms such as the double adaptive bandlimited multiple Fourier linear combiner provide better estimation accuracy [49], in this study, a WFLC was adopted due to its lower computational cost [50]. Here, the WFLC was used to estimate the first harmonic dominant frequency. Equation (1) represents the time-varying sinusoidal term of the Fourier series, where M defines the number of harmonic frequencies for that model. At the discrete-time index k, the estimate $\hat{s}_{i_k}$ in (2) of the input signal s_k (corresponding to $\dot{\varphi}_{\text{tremor}}$) is calculated. Equation (3) defines the error between the input signal and the estimate. A least squares algorithm updates the estimates of dominant frequency ω_{0_k} and the weight vector w_k using this error term in (4) and (5). The adaptation terms μ_0, for the frequency ω_0, and μ_1, for the weight vector w_k affect the tracking ability and stability of the estimation.

$$x_{r_k} = \begin{cases} \sin\left(r \sum_{t=1}^{k} w_{0_t}\right), 1 \le r \le M \\ \cos\left(r \sum_{t=1}^{k} w_{0_t}\right), M+1 \le r \le 2M \end{cases} \quad (1)$$

$$\hat{s}_{i_k} = w_k^T x_k \quad (2)$$

$$\varepsilon_k = s_k - \hat{s}_{i_k} \quad (3)$$

$$\omega_{0_{k+1}} = \omega_{0_k} + 2\mu_0 \varepsilon_k \left(w_{1_k} x_{2_k} - w_{2_k} x_{1_k}\right) \quad (4)$$

$$w_{k+1} = w_k + 2\mu_1 x_k \varepsilon_k. \quad (5)$$

Here, the number of harmonic frequencies M of the model was fixed to 1 as only the first harmonic frequency, the tremor frequency, was targeted. The adaptations term were determined in preliminary experiments and set to $\mu_0 = 2 \cdot 10^{-7}$ and $\mu_1 = 0.01$ with a starting frequency $\omega_{0_{k=0}}$=6Hz.

The power of tremorous movements is smaller than that of voluntary origin which is why the WFLC can converge towards the voluntary component [48]. Therefore, the tremor signal needed to be isolated from voluntary movements originating from the wrist, and as we were using only one sensor, also from other motions of the body measured at the hand. An estimation of the voluntary movement component was subtracted from the sensory signal to generate the isolated tremor signal. Here, a Kalman filter was chosen, as

it is a widespread estimation algorithm for real-time human motion tracking [51], [52].The Kalman filter is separated into two update states: the time update and the measurement update [53], [54]. The time update (6) and (7) were responsible for projecting forward in time and obtaining an estimate of the state at the next time step, acting as a predictor. The measurement updated (8), (9), and (10) incorporating the new measurement to improve the estimate, acting as a corrector where

- A_k is the state-transition model,
- H_k the observation model,
- K the updated Kalman gain,
- Q_k the covariance of the process noise,
- R_k the covariance of the observation noise and
- B the control input model which applies to
- u_k, the control vector.

$$\widehat{x_{k+1}^-} = A_k\widehat{x}_k + Bu_k \tag{6}$$

$$P_{k+1}^- = A_k P_k A_k^T + Q_k \tag{7}$$

The updated state $\widehat{x}_k$ was an estimate at the time k based on the actual measurement z_k (corresponding to $\dot{\varphi}_{\text{sensor}}$). P_k was the estimated covariance matrix, a measure for the estimated accuracy of the state estimate.

The state-transition model was set to A=[1, T; 0, 1], the process noise vector covariance matrix to Q=[0, 0; 0, 0.0125]*T) whereas T the sample time was. The measurement noise vector covariance was dimensioned to R=0.0643 based on preliminary experiments.

$$K_k = P_k^- H_k^T \left(H_k P_k^- H_k^T + R_k\right)^{-1} \tag{8}$$

$$\widehat{x}_k = \widehat{x_k^-} + K_k(z_k - H_k\widehat{x_k^-}) \tag{9}$$

$$P_k = (I - K_k H_k)P_k^- \tag{10}$$

The Suppression Controller created a step voltage signal u_c for the brake, based on the zero-crossing of the estimated tremor signal $\hat{s}_{i_p}$ of the WFLC, where p is a future time step of the prediction. Here, the length of the step signal was adjusted, as well as the delay time. The delay time was timing as a percentage of the tremor cycle calculated from the tremor frequency ω_{0_k} in which the brake was activated. The tremor prediction time was set to 13ms as the brake needed 13ms to close.

As the step signal duration and delay time needed to be adjusted with 1ms range, the Suppression Controller had a sampling frequency of 1000Hz The sampling frequency of the gyroscope, Kalman filter, and WFLC was 200Hz, which is high enough for tremor assessment and processing (1000Hz was not possible due to the capabilities of the gyro sensor).

C. System Model

When evaluating a tremor suppression mechanism, it is advantageous to simulate the human input to improve the performance of the system before human trials [55], [56], [57]. Here, we designed a computational simulation and validated the results with a test bench to determine the optimal brake duration and delay time. For the computational simulation and test bench, the human joint was simplified as a 1 DOF with only wrist flexion-extension. The controlled brake was attached to this modelled human joint to determine the optimal parameter and investigate the tremor suppression efficacy of the mechanism. The optimum was here defined as the maximum of tremor suppression whilst minimum voluntary movement suppression.

The human muscles can be compared to viscoelastic structures, as they are involved in damping [58]. Therefore, the human system was modelled as a spring-damper with a rotary mass. Even though reflexes can modulate the viscous and elastic components of the mechanical impedance provided by the muscle [59], we assume that this effect was neglectable and simplified the human as an open-loop system without any changes in the impedance or planned trajectory (as it was done in numerous publications [30], [31], [32], [33], [34], [35], [47], [56], [57], [60], [61], [62], [63], [64], [65]). The rotary mass inertia J_H of the human hand was set to 0.00285Nms2/rad, the damping B_H to 0.04Nms/rad, and stiffness K_H to 1Nm/rad, according to the literature [47], [56], [60], [61], [62].

D. Computational Model

A 1-DOF model of the human wrist as well as of the control system with brake was designed using MATLAB Simulink (R2021a, The MathWorks Inc., MA, USA) (see Fig. 3). The brake was implemented into the computational model as a logic-controlled friction clutch with a friction torque of 0.2Nm. The wrist was modelled as a rope drum with a radius of 30mm connected to the brake, which had a radius of 6mm with idealized ropes (torque transmission ration r=1/5). The lever of 30mm at which the rope was connected to the wrist was an estimate based on anthropometric data and which also corresponded to literature [66]. The rotary mass was also connected to a rotary spring and damper simulating the wrist impedance. The wrist, brake, rope, spring and damper were modelled using Simscape mechanica blocks. The Kalman filter was implemented into Simulink after Busarello and Simões [67].

E. Test Bench

The test bench incorporated the same controller, rope and brake used in the orthosis. With the test bench, the simulated brake mechanism with the control loop was validated with the actual elements used with the orthosis. The human model was incorporated into the test bench with a physical rotating mass actuated by a motor and a virtual spring-damper (hybrid human model). The rotating mass had the defined mass of inertia of the hand model, including the drivetrain consisting of electrical motor, gear, shaft and encoder. The electric motor (DCX 35 L, Maxon Motor AG, Obwalden, Switzerland) was connected by the gear with a transmission ration of 3.9 (GPX 37, Maxon Motor AG, Obwalden, Switzerland) to the encoder with 2000 increments (8661-5005-V0400 with angle measurement, Burster Präzisionsmesstechnik GmbH & Co. KG, Germany) (see Fig. 4). The motor was torque controlled by the microcontroller on a higher level, with an interface to LabVIEW (LabVIEW Full Development System 2019.0.1f1 (32bit), National Instruments Corp., TX, USA)

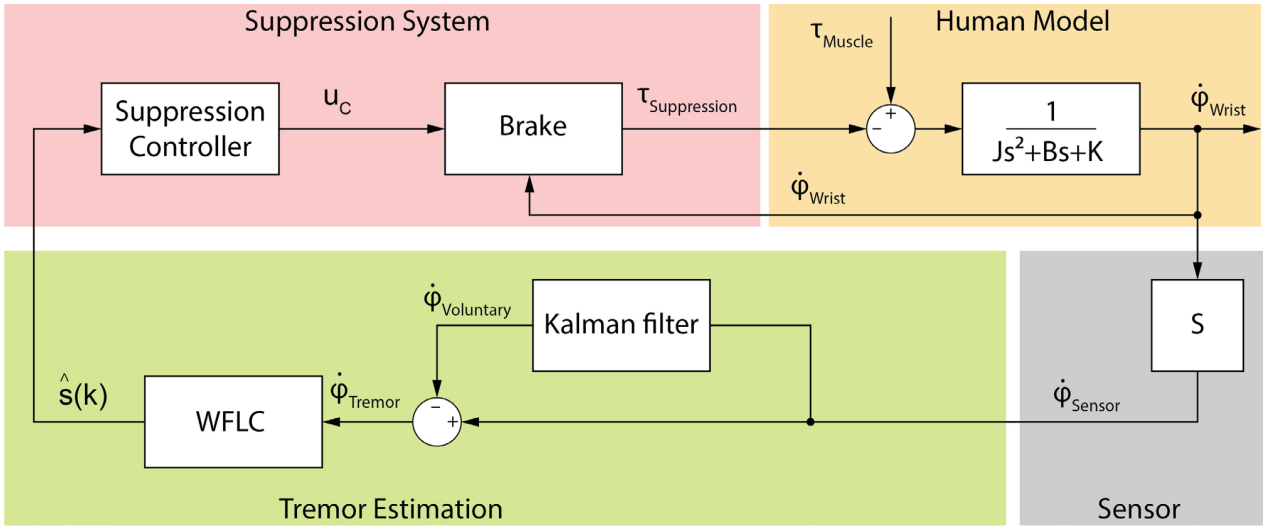

Fig. 3. Control scheme of simulation. The Kalman filter combined with the WFLC provided a dynamic tremor estimation model ŝ(k) based on the angular velocity $\dot{\varphi}_{sensor}$ received from the human model. The suppression controller triggered the step signal based on the zero-crossing of the predicted tremor estimation model and delayed the onset based on the adjustable tremor delay time parameter. This controller adjusted the length of the brake voltage step signal u_c based on the brake duration parameter. A defined torque, a combination of tremorous and voluntary movements, interacted with the human model.

where a defined torque profile was read into. The microcontroller also received position measurement from the hall sensor with which the virtual spring and damper were implemented (see Fig. 5). On the lower level, the motor was controlled by a motor controller (EPOS4 Compact 50/5 CAN, Maxon Motor AG, Obwalden, Switzerland) running at 50kHz for current control.

$$H(s) = \frac{\varphi(s)}{\tau_d(s)} = \frac{1}{J_H s^2 + B_H s + K_H} \tag{11}$$

$$P(s) = \frac{\varphi(s)}{\tau_d(s)} = \frac{1}{J_H s^2 + (B_H + B_P)s + K_H + K_P} \tag{12}$$

$$G(s) = \frac{\varphi(s)}{\tau_d(s)} = \frac{1}{J_H s^2 + (B_H + B_{SA}(c))s + K_H} \tag{13}$$

F. System Dynamics Determination

The impact of the mechanism (controlled brake) on the human wrist joint dynamics was analyzed with special emphasis for the range of voluntary movements, below 2Hz, and tremorous movements between 3Hz and 12Hz. Therefore, the system dynamics of the raw human wrist joint were determined and compared to the one of the human wrist joint in the controlled loop interacting with the brake.

Depicting the system dynamics of the mechanism, bode plots of the adaptive control loop transfer-function, including the human dynamics, were generated by determining the system response of a sinusoidal input disturbance torque (instead of the muscle torque) at the frequencies between 0.1Hz to 15Hz. With a discrete Fourier transformation, the change in amplitude magnitude was calculated, comparing the input signal (torque) with the output signal (position) at the given frequency. Additionally, the phase shift of the output signal compared to the input signal was calculated. The phase shift was plotted only for the frequencies of the disturbance torque at which voluntary movements occur, as a phase shift influenced primary voluntary movements. A phase shift in tremorous frequencies was not relevant so they were not depicted.

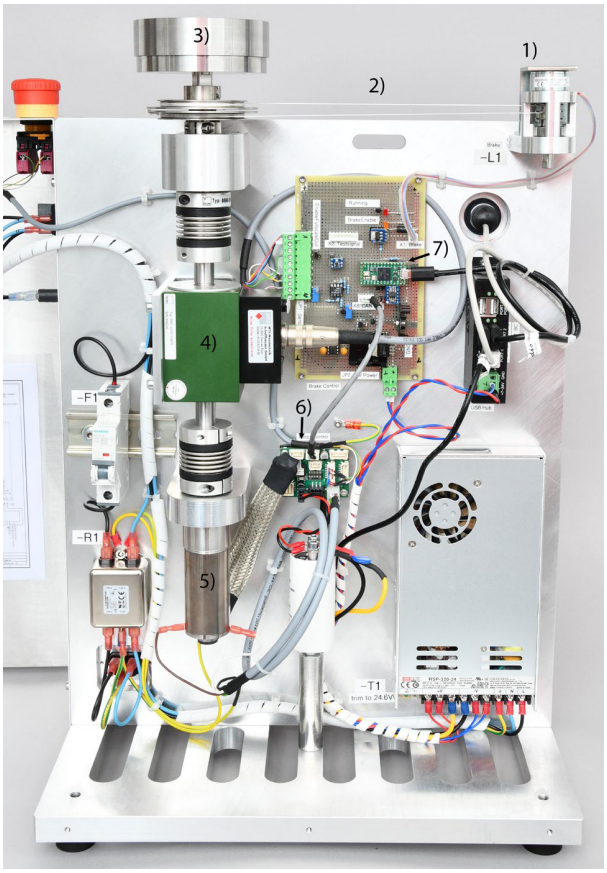

Fig. 4. Test bench setup with rotary mass 3) connected to the brake 1) via the rope 2). The rotary mass 3) was coupled to the motor with gear and hall sensor 5) through the encoder 4). The motor 5) was controlled on the low level by the motor controller 6) and on the high level by the microcontroller 7), which also estimated the tremor and controlled the brake 1).

TABLE II
HUMAN JOINT DYNAMICS AND SPRING-DAMPER VALUES OF PASSIVE DAMPING MECHANISMS FROM LITERATURE FOR THE TRANSFER FUNCTIONS P(S)

	$P_1(s)$ Katz 2017 [73]	$P_2(s)$ Takanokura et al. 2011 [66]	$P_3(s)$ Kotovsky and Rosen 1998 [26]
B_P (in Nms/rad)	0.12	1.62 (1.8kNs/m at 30mm)	0.12
K_P (in Nm/rad)	0	0	2.35
J_H (in Nms^2/rad)	0.00285	0.00285	0.00285
B_H (in Nms/rad)	0.04	0.04	0.04
K_H (in Nm/rad)	1.0	1.0	1.0

The system dynamics of the raw human joint served as a point of reference for the system dynamics with the interfering tremor suppression mechanism. Here, the human joints system was modelled as a continuous-time all-pole second-order transfer function H(s) as in (11). Our brake was seen as a damper function of the controller $B_{SA}(c)$ which was represented as second-order transfer function G(s) as in (13). To calculate the system response of the mechanism, the adaptive controller was restricted to one fixed frequency of 6Hz, mimicking a tremor frequency. This served the purpose that the impact of the semi-active system on the surrounding frequencies was visible. A second system response of the controlled brake being adaptive (free) was calculated, representing the adaptability of the controller and efficacy of the mechanism at all frequencies. The brake duration and delay time of the controller were selected based on the determined optimum parameter.

Additionally, passive tremor suppression systems based on literature values were modelled as a second point of reference. The human transfer function H(s) was extended with spring-damper values BP and KP (see Table II), resulting in the new continuous-time all-pole second-order transfer function P(s) in (12).

The simulated system response of the controlled brake with the human joint model G(s) as well as the response of the modelled human joint system H(s) was validated with the test bench (G′(s) and H′(s)).

G. Controller Parameter Determination

1) System Dynamics: The brake and suppression control were designed to close the brake periodically for an optimized duration and at the optimal delay time in the sinusoidal tremor cycle of the dominant frequency while not influencing the other frequencies. One objective (O1) of this study was to determine the optimal duration and delay time. Therefore, the system dynamics for the different control parameters were investigated. Bode plots of the adaptive control loop transfer-function G(s) for a variety of control settings were generated with the computational model. To investigate the influence of the delay time parameter on the system dynamics, the brake duration was set to 25ms, a point of reference from Herrnstadt and Menon [36], whereas the delay time was adjusted between 0%, 5%, 10%, 20%, and 30%. To investigate the influence of brake duration on the system dynamics, the delay time was set to 5% and the brake duration adjusted between 5ms, 10ms, 20ms, 25ms, 30ms, and 40ms.

2) Tremor Simulation: To identify the optimal control parameter with a two-state suppression mechanism, measured tremorous movement data were used to run the computational model. Here, the optimum was defined as the maximum tremor suppression and minimum voluntary movement suppression. Timmer et al. attached accelerometers to the dorsum of the outstretched hand to measure and analyze pathological tremor [68].

Those movement data from five ET and five PD participants were used to compute the generated torque by the muscles to execute the measured movement, using the inverse dynamics of the human wrist joint. With those torques, the tremor and voluntary movement suppression for different control parameters were determined. The system model behaviour was simulated with all combinations of control parameters of the brake duration of 0ms to 100ms in 1ms steps and delay time of 0% to 50% in 1% steps, leading to 5151 simulations per participant data. From those simulations, tremor and voluntary movement suppression heat maps were perceived for each tremor dataset. The optimum parameter was computed by first creating a new heat map subtracting the mapped percentual tremor suppression from the mapped voluntary movement suppression and adding 100% for positive values (referred as Voluntary-Tremor+100), and second finding the minimum of this subtraction map.

The optimum brake duration and delay time, determined by the computation model for each dataset, were validated in a cross-section method on the test bench. Therefore, the optimum brake duration was combined with the delay times of 0% to 50% in 5% steps, and the optimum delay time combined with the brake duration of 0ms to 100ms in 5ms steps. The cross-section method, exemplary, for the first ET participant dataset, ET01, was run five times on the test bench to depict its variability. Furthermore, the randomly selected dataset ET01 was validated on the test bench with all combinations with a delay time of 0% to 50% in 5% and brake duration of 0ms to 100ms in 5ms steps. Here, only one dataset was selected to limit the number of runs on the test bench.

The tremor suppression efficacy was determined by calculating the power spectral density (PSD). This determines the

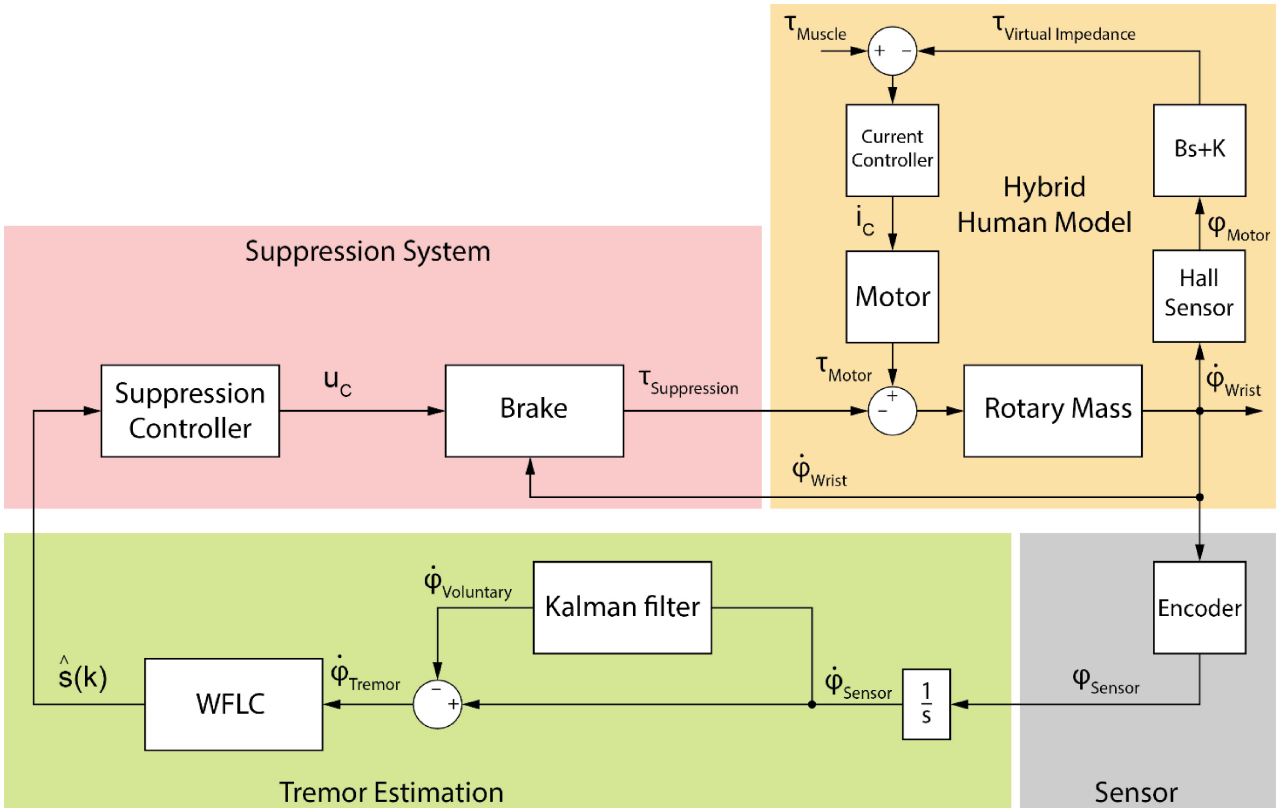

Fig. 5. Control scheme of the test bench. The Kalman filter combined with the WFLC provided a dynamic tremor estimation model ŝ(k) based on the angular velocity $\dot{\varphi}_{\text{sensor}}$ received from the hybrid human model (physical and virtual impedance). The suppression controller triggered the step signal based on the zero-crossing of the predicted tremor estimation model and delayed the onset based on the adjustable tremor delay time parameter. This controller adjusted the length of the brake voltage step signal uc based on the brake duration parameter. The motor applied a defined torque, a combination of tremorous and voluntary movements, accelerating the rotary mass. Based on the position measured by the hall sensor, was a virtual spring-damper calculated and subtracted from the defined torque in a feedback loop.

tremor power, defined as the power of the angular acceleration (derivative of the angular velocity measured by the gyro sensor) deg^2/s^3 over its frequency in Hertz, plotted as in dB. The PSD was calculated using the Welch-Bartlett Method (based on fast Fourier transform) using a 50% overlap of 500 sample Hamming windows [23], [69], which is the most common method for tremor analysis [70]. To determine the power suppression of tremor and voluntary movements, the dominant tremor power frequency was identified in the range of 3Hz to 12Hz [4] for an activated and deactivated mechanism. The difference in PSD between the activated and deactivated mechanism was converted to a tremor suppression percentage.

The impact of the tremor suppression mechanism on voluntary movements are often determined by calculating its power as it is done for tremor, but in the range below 2Hz for voluntary movements [40]. However, even if the PSD of the voluntary movement is the same, the trajectory can be different compared to the intended one, for example, with a delay. Any difference compared to the planned trajectory is perceived as a disturbance of voluntary movements by the human. For the computational simulation and the test bench, we defined the suppression of voluntary movements by the distance between the intended trajectory and the executed trajectory as in (14) [71], whereas the distance of no movements, m_{fixed}, corresponds to 100% as in (15).

$$m = \frac{1}{n}\sum_{i=1}^{n} d_i \tag{14}$$

$$V = \frac{m_{\text{clutch}}}{m_{\text{fixed}}} \cdot 100\ \% \tag{15}$$

H. Orthosis Proof-of-Concept Verification Study

The objective (O2) of this study was to evaluate a semi-active, textile-based orthosis with one tremor affected participant in activities of daily living, differentiating between the performed tasks.

One experimental session (1 hour) included three sequences of measurements. Each sequence included the same set of tasks of daily living. One sequence was performed with the orthosis in the inactive state. The other two sequences were performed with the orthosis active but with two different pairs of control settings. One pair of control settings, i.e., braking duration and delay time, represented the optimum determined in the simulations, the other setting was a randomly chosen pair that performed worse in the simulations.

The performed tasks were part of the standardized motor tasks of the WHIGET Tremor Rating Scale Test [72], which is used for clinical tremor rating. The chosen tasks included drinking from a cup full of water (Drinking), pouring water

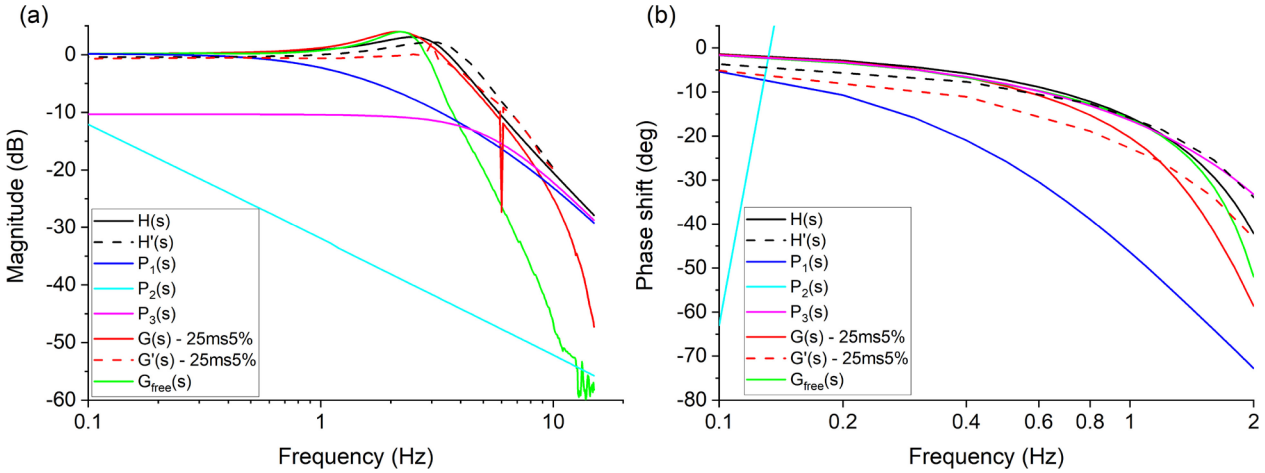

Fig. 6. Bode plot with change in magnitude in (a) and phase shift over the frequency w in (b). The modelled human joint dynamic second-order transfer function H(s) as well as the measured system dynamics on the testbench H'(s). The passive suppression transfer functions $P_1(s)$, $P_2(s)$, and $P_3(s)$ were modelled. The system dynamics G(s) with 25ms brake duration and 5% delay time as well the corresponding test bench dynamics G'(s) and the free controller system dynamics $G_{free}(s)$ were depicted.

TABLE III
QUESTIONNAIRE (QUESTIONS REGARDING THE ORTHOSIS IN GENERAL AND FOR EACH PART OF THE TESTS: INACTIVE, ACTIVE 1 AND ACTIVE 2)

Section	Question no.	Question	Rating
General	Q1	The orthosis is light and doesn't disturb	1-6
	Q2	The orthosis is optically appealing	1-6
	Q3	Would you wear the orthosis	1-6
Test x	Q1	Does the orthosis hinder voluntary movements	1-6
	Q2	The orthosis reduces the tremor	1-6
	Q3	The orthosis is comfortable	1-6

Rating 1(disagree/negative) – 6 (agree/positive).

into a cup from a 0,5l bottle (Pouring), spooning water from a bowl up to the mouth (Spoon-Up) and following an Archimedes spiral on a paper with a pencil (Drawing-Spiral). Each task was repeated five times to generate a task average. The different tasks in a sequence were completed in a randomized order.

The gyroscope at the hand from the orthosis was used for motion tracking. The angular velocities for the hand angles were sampled at a rate of 200Hz. The signal was filtered with a high-pass Butterworth filter at 0.1Hz and a low-pass Butterworth filter at 15Hz to remove movement artefacts. Furthermore, the PSD for the wrist radial-ulnar deviation, wrist flexion-extension, and pronation-supination was calculated. The tremor power suppression and voluntary movement suppression in the PSD were calculated using the same method used in the parameter determination for the wrist flexion-extension, pronation-supination and radial-ulnar deviation.

After the session, a questionnaire was answered investigating the impairment of voluntary movements and comfort of the orthosis for the three sequences (see Table III). Additionally, it was asked if the appearance of the orthosis pleases and if the orthosis would be worn. A numeric rating scale from 1 to 6, where 6 is good or agree and 1 bad or disagree, was chosen. The scale corresponds to the school system grading (Switzerland) and was therewith easy relatable for our participants.

The study was conducted with one ET affected participant, aged 69 years. The participant was free of any other condition affecting upper limb movements or motor control (e.g., spasticity, paralysis or muscular insufficiency) and had no known injuries or illnesses that may have affected safe participation.

For the data post-processing MATLAB (R2021a, The MathWorks Inc., MA, USA) was used. Due to the small sample size, no statistical test was conducted. Instead, the 95% confidence intervals for the mean of each task in each sequence were calculated from the repetition under the assumption of a normally distributed population. The data distribution and confidence intervals were graphically analyzed using a boxplot. Here, the box represents the standard deviation with a mark for the mean, while the whiskers represent the 95% confidence interval. Non-overlapping confidence intervals indicated a possible difference between the datasets.

The study and experimental protocol were designed in accordance with the Swiss Federal Act on Research involving Human Beings. The measurements were approved by the ethics commission of ETH Zurich in accordance with the Declaration of Helsinki (EK 2021-N-164). The participant volunteered and gave written informed consent to participate in the study.

III. RESULTS

A. System Dynamics

The system dynamics, in the form of a Bode plot, of the test bench and computational simulation behaved similarly to the modelled second-order transfer function of the raw human wrist joint H(s) (Fig. 6). The semi-active mechanism, with the controller fixed to 6Hz, showed a drop at 6Hz of 15.7dB for the computational simulation G(s) and 19.6dB for the test bench G'(s) compared to the corresponding wrist dynamics H(s), equivalent to 83.6% and 89.5% reduction of amplitude at 6Hz. The maximum deviation of amplitude of G(s) in the

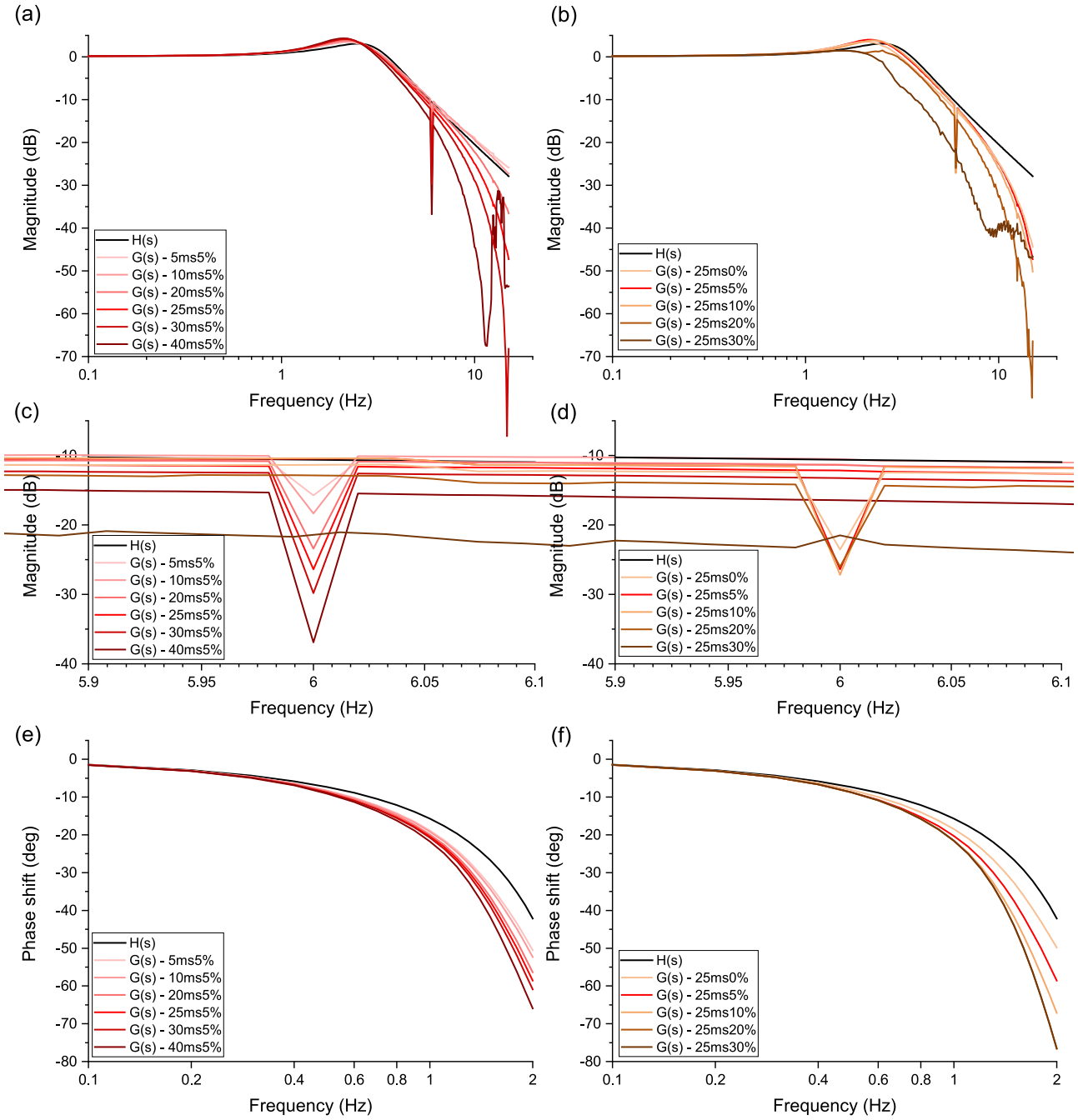

Fig. 7. System dynamics parameter comparison. (a) and (b) presents the change in magnitude of G(s) for different parameters compared to the human modelled dynamics H(s). (c) and (d) presents the changed magnitude in the frequency of 6Hz. In (e) and (f) are the phase shifts of the system dynamics. Different brake duration at 5% delay time was compared in (a), (c) and (e). Different delay times at 25ms brake duration were compared in (b), (d) and (f).

range of voluntary movements, below 2Hz, was an increase of 1.9dB (19.7%) at 2Hz. The phase shift in the computational simulation and test bench diverged with increasing frequency with up to 16.4° and 9.9° at 2Hz, respectively. The dynamics Gfree(s), where the controller adapted to the frequency, provided the maximum tremor reduction for each frequency. The dynamics of the passive suppression systems P1(s) [73], P2(s) [66], and P3(s) [26] lowered the magnitude at 6Hz by 6.03dB (50.1%), 37.35dB (98.6%) and 5.15dB (44.7%).

B. Controller Parameter Determination

The system dynamics for the different control parameters derived from computer simulation were depicted with a Bode plot (see Fig. 7).

1) Brake Duration: The brake duration parameter had a primary impact on the tremor suppression compared to the impact of the delay time. The longer the brake was activated, the more tremor amplidute was suppressed. A brake duration of 5ms, at the delay time of 5%, reduced the amplitude magnitude at 6Hz by 5dB (47.8%), while a brake duration of

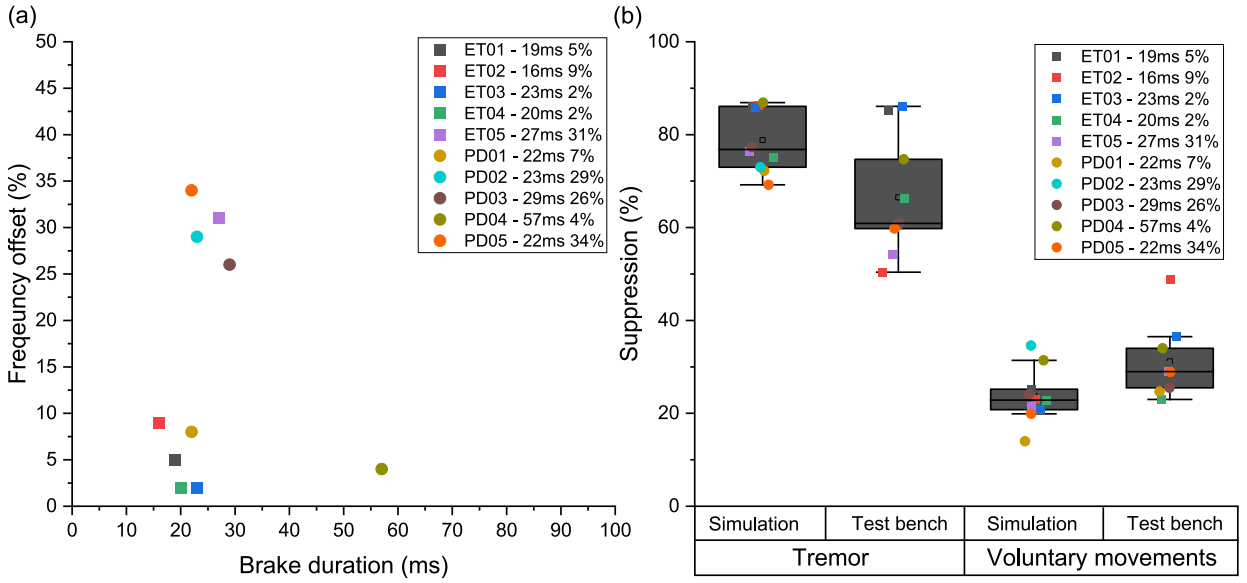

Fig. 8. Overview of simulation results. (a) the optimal parameter for the five ET and PD datasets resulting from the computational simulation. (b) the resulting tremor and voluntary movements suppression in computational and test bench simulation for all datasets.

40ms reduced the amplitude by 21.7dB (91.8%). The longer the brake duration, the more amplitude suppression were also recorded in the frequency of voluntary movements, below 2Hz, ranging between 0.7dB and 1.7dB (7.8% and 17.9%, respectively). A phase shift between 8.3° at 5ms and 23.7° at 40ms was recorded at the system output.

2) Delay Time: The delay time had a stronger influence on the phase shift of voluntary movements compared to the brake duration. At 2Hz, the phase was shifted by 7.6° for 0% offset and 34.4° for 30% delay time (while simulating a brake duration of 25ms). The amplitude magnitude at 2Hz was changed by 1dB at 0% offset and 1.7dB at 30% offset, corresponding to 10.8% and 17.9%. The tremor amplitude of 6Hz was reduced by 16.5dB (85.1%) for 5%, 10%, and 20% delay time. An offset of 0% was, in comparison, less amplitude reducing with 12.9dB (77.4%) to 30% delay time suppression 10.9dB (71.5%) tremor amplitude.

The optimum regarding maximum tremor suppression and minimal voluntary movement suppression was determined for those datasets (see Fig. 8). The computationally simulated tremor suppression with the optimized parameter was in mean 78.8% (from 69.2% to 86.9%), with a mean voluntary movement suppression of 23.7% (from 14.0% up to 34.6%). The optimal parameter varied between the datasets, whereas all data sets except PD04 had the optimum brake duration between 16ms and 29ms. The optimum delay time was either between 2% and 9% or between 26% and 34%. The mean tremor suppression determined with the test bench was 66.5% (from 50.4% to 86.1%), while the voluntary movement tremor suppression was 32.2% (from 23.0% to 36.5%).

Compared to the different passive suppression mechanisms, running the simulation with the dataset ET01 (exemplary dataset), our proposed semi-active system suppressed more tremor energy while preserving more voluntary movements (see Fig. 9).

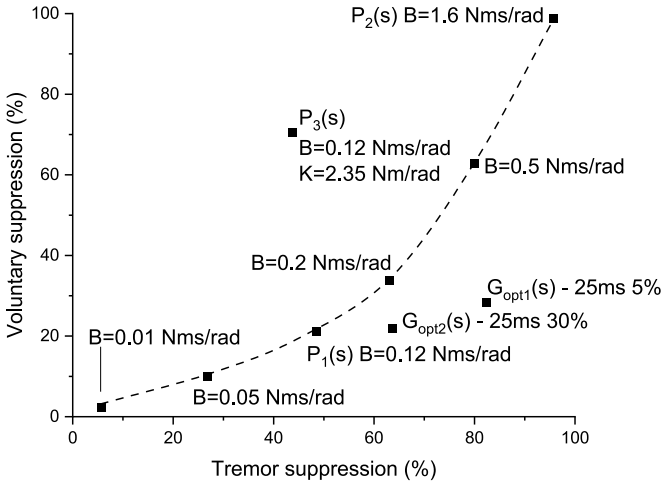

Fig. 9. Comparison of passive tremor suppression to controlled, two-state suppression G(s) on the dataset of ET01. $G_{opt1}(s)$ and $G_{opt2}(s)$ are the two identified parameter optima. Passive linear dampers without spring were connected with a dotted line where the damping constant B increases from left to right.

The computational simulations were Verified with a test bench for the dataset ET01 (see Fig. 10). Verifying the simulation results with the test bench in the cross-section method confirmed the outcome of the simulation regarding brake duration, especially for durations up to 50ms (see Fig. 11). Brake duration higher than 50ms caused a higher suppression of voluntary movements on the test bench compared to the simulation. The test bench results of the cross-section method for ET01 had a standard variation between 0.2% and 3.7% suppression.

The root-mean-square (RMS) error between the test bench and simulation was between 22.8% and 39.6% for the voluntary movements and between 3.6% and 8.8% for tremor with a fixed delay time. The RMS for fixed brake duration was between 4.2% and 21.7% for voluntary movements and between 10.9% and 22.4% for tremor.

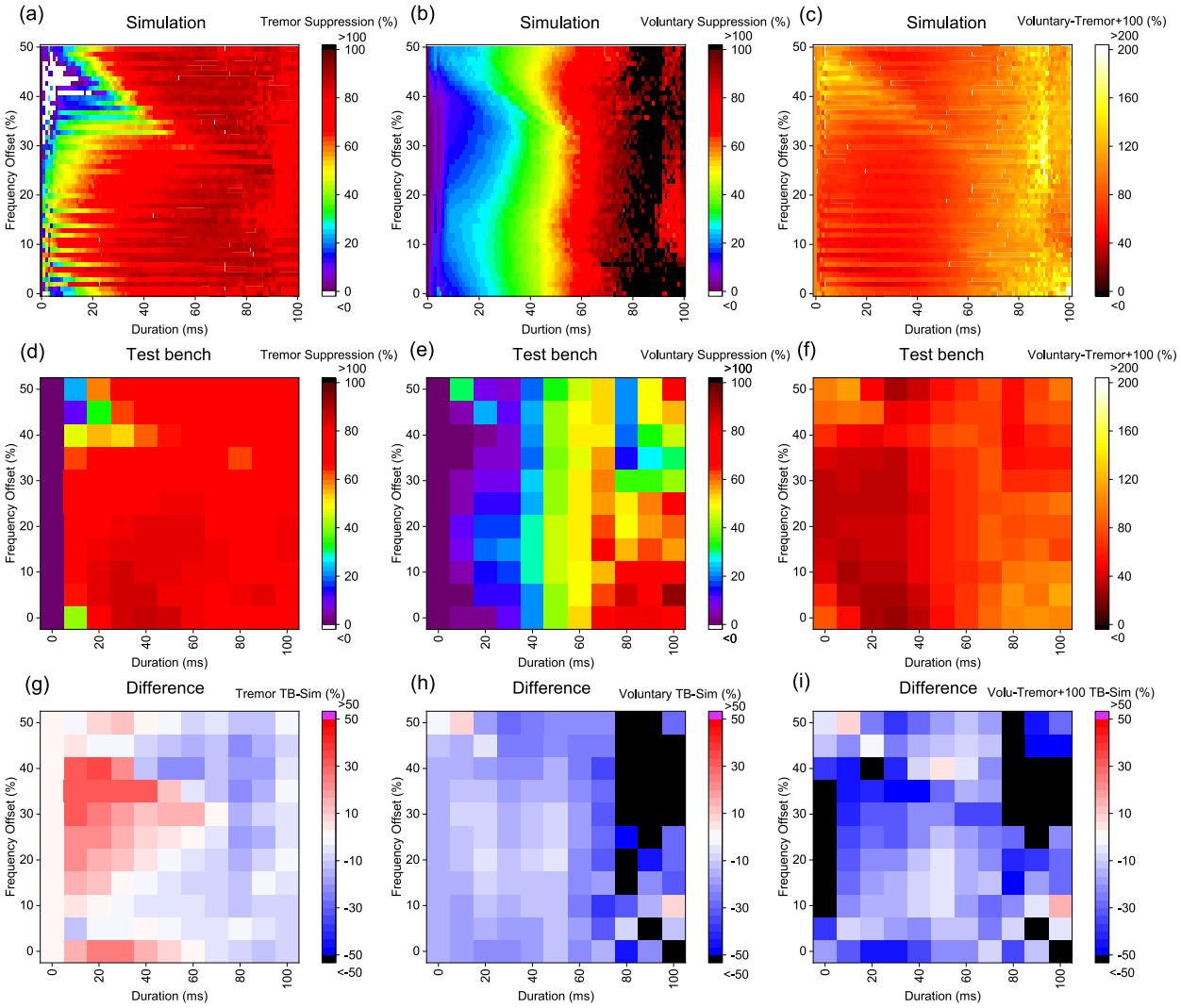

Fig. 10. Computational simulation compared to test bench. (a), (b), and (c) the computational results. (d), (e), and (f) the test bench simulation results. (g), (h), and (i) the difference between the computer and test bench. In (a) & (d) the tremor suppression, (b) & (e) the voluntary movement suppression and (c) & (f) the Voluntary-Tremor+100% to identify the optimum for the combinations of brake duration and delay time.

C. Orthosis Proof-of-Concept Verification Study

The PSD of the participant's hand movement was depicted for the different tasks of wrist flexion-extension, pronation-supination, and radial-ulnar deviation, between orthosis off and orthosis on with optimal parameter with a brake duration of 25ms and delay time of 5% (see Fig. 12). The PSD of the wrist flexion-extension with the orthosis brake on the optimum parameters showed a possible difference in tremor compared to orthosis brake off (because of non-overlapping confidence intervals) for the tasks Drinking, Pouring and Drawing-Spiral by 41.1%, 55.3% and 26.0%, respectively (see Fig. 13 and Table IV). Comparison of the drawn spirals with the orthosis brake turned on and off by eye did not show a visual difference. No difference was recorded between the orthosis bad parameter and orthoses off. Furthermore, neither with optimum parameter nor with bad parameter were the voluntary movement power impaired.

The participant rated the orthosis when turned off as well as turned on with both settings not impairing voluntary movements (rated 5 out of 6 where 1 means disagree and 6 agree). The participant rated the orthosis for all cases as comfortable (rated 5 out of 6). In general, the participant rated the orthosis as lightweight and unobtrusive (rated 5 out of 6) and stated that the orthosis would be worn (rated 6 out of 6). The appearance of the orthosis did not please the participant and was rated 1 out of 6.

IV. Discussion

A. Control Parameter and Efficacy

1) Simulation Validation: The design of the human model as a linear 1 DOF spring-mass-damper representing only wrist flexion-extension impedance, neglecting radial-ulnar deviation and pronation supination was a simplification of our modelled system. The wrist impedance is non-linear and depends on the position [74], [75]. A radial or ulnar deviation of the wrist will change the impedance in flexion-extension. However, this simplification is a common method in the literature. Our proposed mechanism, including the control strategy, functions independently of any prior knowledge of the joint impedance

TABLE IV
OVERVIEW OF MEAN AND LIMITS OF THE 95% CONFIDENCE INTERVAL FOR THE DIFFERENT TASKS AND THEIR CONDITIONS

Task	Condition	Tremor power (dB)			Voluntary movement power (dB)		
		Upper Limit	Mean	Lower Limit	Upper Limit	Mean	Lower Limit
Drinking	Off	39.4	37.3	35.1	22.6	17.5	12.4
	Opt	34.4	32.6	30.8	17.3	12.0	6.7
	Bad	37.7	34.6	31.4	22.3	14.9	7.5
Pouring	Off	41.5	37.0	32.4	11.6	9.2	6.8
	Opt	31.1	29.5	27.9	15.8	9.3	2.7
	Bad	37.6	35.6	33.6	18.1	12.3	6.4
Drawing-Sprial	Off	33.1	31.6	30.1	20.6	19.3	17.9
	Opt	29.8	29.0	28.3	21.3	16.9	12.5
	Bad	31.6	29.6	27.7	23.8	17.1	10.4
Spoon-Up	Off	45.9	41.4	36.9	27.2	22.7	18.2
	Opt	44.6	39.9	35.2	22.9	18.5	14.0
	Bad	42.7	38.6	34.5	23.4	17.1	10.9

as it simply modifies the impedance by adding a damping component. The prevailing joint impedance, linear or non-linear, does not influence the added damping. Taheri et al. proved with their semi-active mechanism that a different joint impedance does not change the amplitude magnitude of tremor suppression [56].

We chose, based on anthropometric data and literature, a lever of 30mm as the connection point to the wrist for this mechanism [66]. The anthropometry varies between individuals changing this lever and therewith also the transmission ratio between the wrist and the brake mechanism. The transmission ratio changes the transmitted torque as well as the transmitted angular velocity of the brake. As the brake can apply 0.2Nm and tremor of up to 0.4Nm can occur in the wrist flexion-extension [31], [35] a lever of at least 12mm (transmission ratio of 2) is required.

While the simulation was a purely virtual, idealized model, the test bench implemented all characteristics from the mechanisms used in the orthosis, which were simplified from the virtual model, e.g., the elasticity of the rope and the friction damping characteristics of the brake. The human model remains simplified in the virtual and physical models.

Compared to the test bench, the setup of the orthosis was influenced by the compliance of the soft tissue, as it is interacting with the human. Therefore, a lower efficacy was expected for human trials.

System Dynamics: The modelled brake mechanism of the simulation needed to be verified with a test bench regarding the validity of its results (O1.2). Therefore, the system dynamics were compared and analyzed, using bode plots, as well the behaviour with tremor datasets.

The measured system dynamics of the test bench H'(s) compared to the modelled transfer function H(s) has a slightly shifted peak of the amplitude magnitude, which represents the eigenfrequency of the system. Else, the system dynamics H'(s) as well G'(s) behaved similar to the modelled H(s) and simulated G(s) in the Bode plot (see Fig. 6). Discrepancies were caused by inaccuracies in the torque output of the system, influenced by the current controller of the motor, play in the gear and friction in the system, which was tried to be compensated. Furthermore, the rotary mass of inertia was calculated based on datasheets where inaccuracies as well neglected inertias (e.g., bearings) may have accumulated to an error.

Despite the small differences in the eigenfrequency, the simulated G′(s) as well as the system dynamics G′(s) of the test bench present the desired notch-filter behaviour at 6Hz (Fig. 6). The analysis of the system dynamics of the test bench provides us with the validity of the computational simulation for the detected optimal parameter combination. Future developments of tremor suppression orthoses can therewith be first designed in a computer simulation to predict their behaviour to then tune the design parameter before building a physical prototype.

Compared to the modelled system dynamics of the wrist in combination with passive tremor absorbers P(s), our presented tremor suppression mechanism G(s) showed a higher amplitude magnitude reduction at tremorous frequencies. Furthermore, the system dynamics G(s) at voluntary frequencies, below 2Hz, had a lower discrepancy to the original wrist dynamics H(s) compared to the passive absorbers from the literature regarding amplitude magnitude. The frequency shift discrepancy was also less compared to the simulated dynamics extracted literature, except P3(s) as a

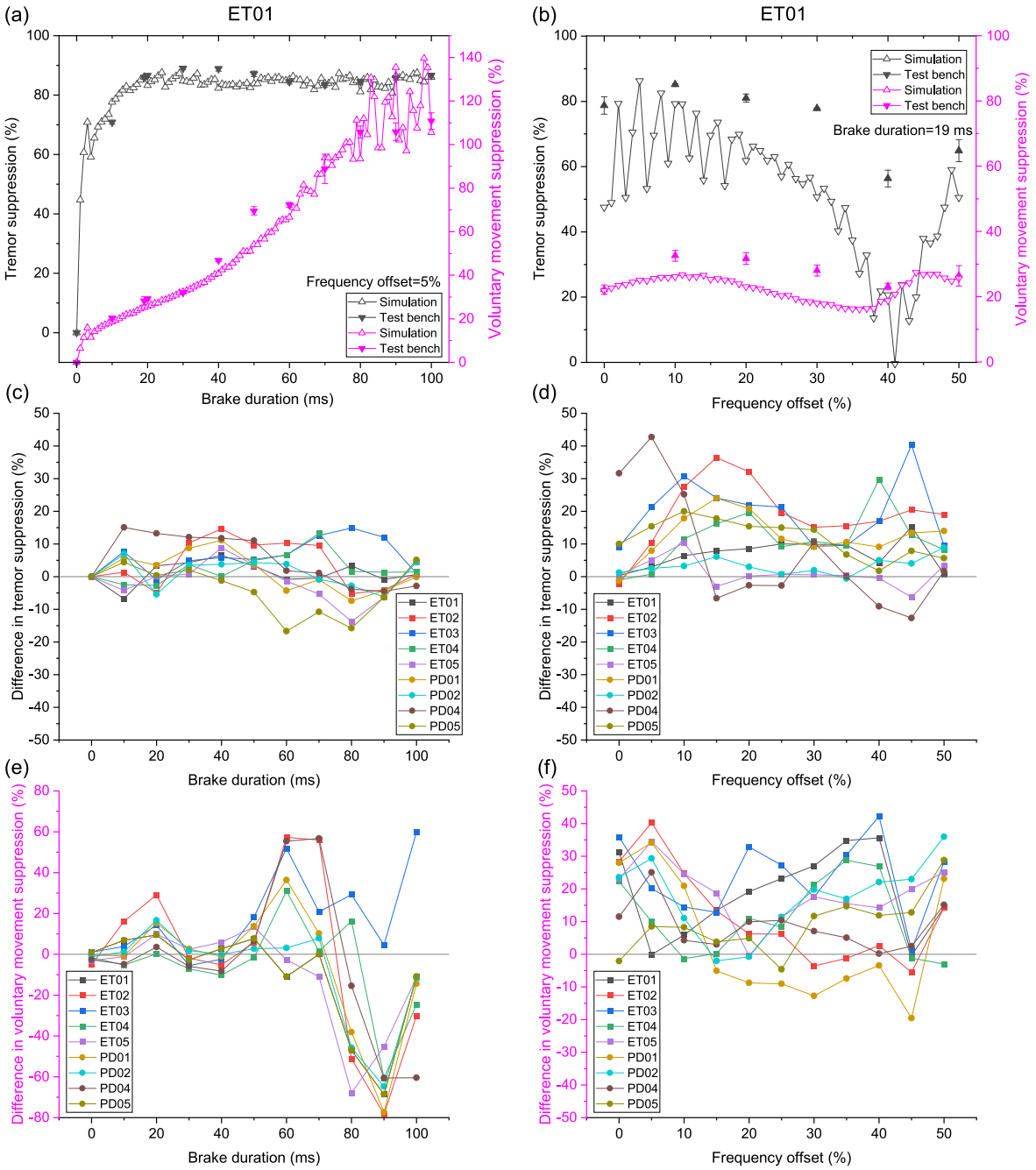

Fig. 11. Cross-section method results. Tremor and voluntary suppression for ET01 determined by computer simulation and test bench with standard deviation for a fixed delay time of 5% (a) and fix brake duration of 19ms (b). Difference between computer simulation and test bench for tremor suppression at fix delay time in (c) and fix brake duration in (d). Difference between computational and test bench for voluntary movement suppression at fix delay time in (e) and fix brake duration in (f). Voluntary movement suppression higher than 100% means that the measured trajectory distance is higher than the one of no movement. Pink Y axis represent voluntary movement suppression whereas the black Y axis shows tremor suppression.

spring was used, which reduced the magnitude by 10dB at low frequencies (see Fig. 6).

Tremor Simulation: Validating the tremor data simulation results with the test bench confirmed the outcome of the simulation regarding brake duration, whereas the delay time deviated more, such that the test bench suppressed more tremor and more voluntary movements. A difference between the simulation and test bench was expected as the test bench included the stiffness of the rope as well as the non-idealized brake. The test bench was also influenced by the play from the gear, which smoothens the sensory read compared to the simulation. This difference generates a different tremor estimate which causes the brake to be activated inaccurately. Analyzing the data qualitatively, an earlier onset of the brake on the test bench compared to the simulation was observed.

The simulation did not depict longer brake duration accurately, especially for voluntary movements (see Fig. 10h and Fig. 11e). This behaviour can be attributed to the missing implementation of the latency time of the brake into the

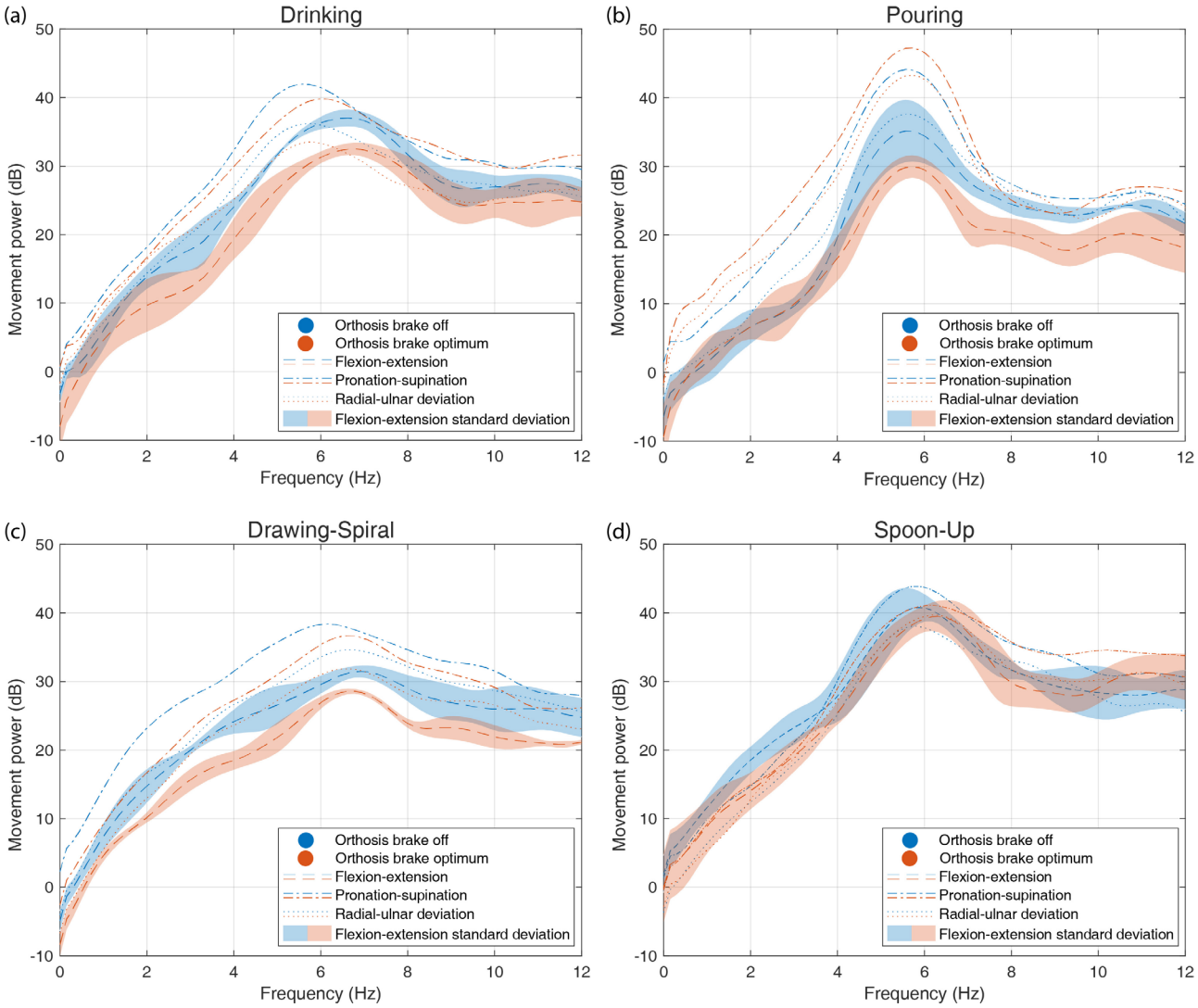

Fig. 12. Movement Power (PSD) of the wrist flexion-extension, pronation-supination and redial-ulnar deviation movement with an orthosis brake turned off (blue) and orthosis brake on (orange) with optimized brake duration of 25ms and delay time of 5% (first optimum) for the task (a) Drinking, (b) Pouring, (c) Drawing-Spiral, and (d) Spoon-Up. For the wrist flexion-extension power the standard deviation is indicated with the shadow.

simulation. It was implemented that the activation of the brake is delayed by 13ms, but for the physical brake on the test bench, the voltage was given 13ms earlier and longer compared to the simulation to build up the magnetic field and close the brake. The observed effect was that the overall activation voltage duration on the test bench, at ca. 80ms, exceeded the tremor cycle duration so the programmed delay time (timing in the cycle) was missed, and it waited for the next cycle. Therewith, the brake skipped every second brake onset compared to the simulation, and more tremor and voluntary movements occurred. This effect was also observed in the simulation but with a higher brake duration, starting at ca. 90ms, as the latency did not add on top (see Fig. 10a & b). The test bench validated the simulation below 80ms by behaving similarly.

2) Parameter Determination: Impedance controllers for tremor suppression commonly rely on assumptions or prior knowledge of the human musculoskeletal system parameter [55], [56], [76]. We applied a WFLC, which did not need to rely on such assumptions or prior knowledge but adapted itself to the different tremor types by predicting the time-varying frequency, amplitude and phase.

Using a gyroscope or acceleration sensor has the limitation that a tremor can never be fully suppressed as the movement is needed to feed the controller with the tremor to stay stable. To overcome this issue future, further improved system can rely on the muscles activities (EMG) as input signal for the controller However, to prevent any instability of the controller, the WFLC frequency was limited to be between 2 to 12Hz which got reset to 6Hz in case of boundary break through.

Herrnstadt and Menon identified the potential disadvantage of a two-state semi-active mechanism of being perceived as uncomfortable by the abrupt interruption of movements [36]. However, they hypothesized that an advanced controller could improve adaptability and help mitigate. Here, the compliance from the orthosis smoothens those abrupt interruptions by the brake, which was confirmed by the gyroscope data. Furthermore, the participant did not report any perception of discomfort related to abrupt interruptions by the brake.

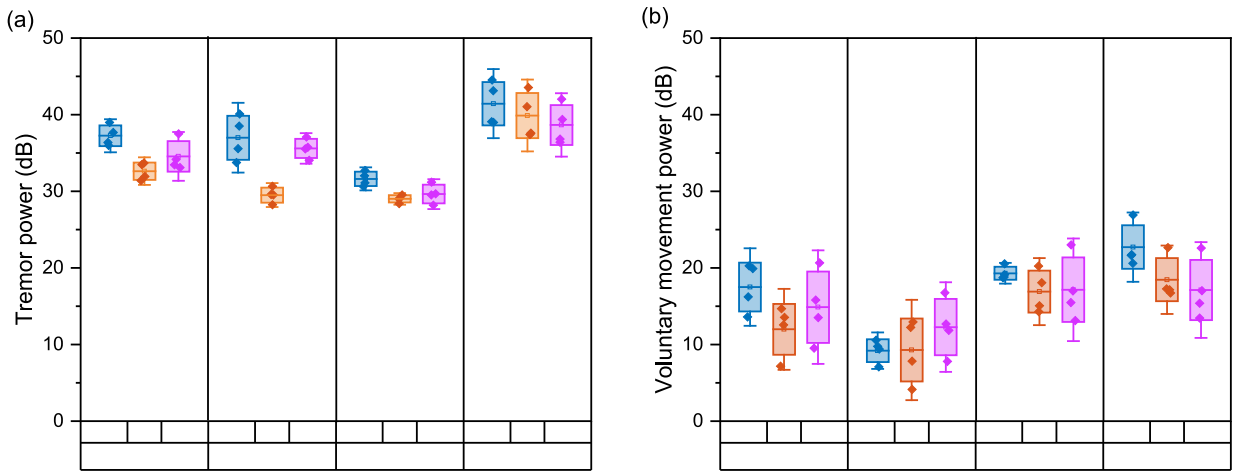

Fig. 13. Movement power comparison. Determined tremor power (a) and voluntary movement power (b) with orthosis brake mechanism off (Off), with orthosis mechanisms on with optimized brake duration of 25ms and delay time of 5% of the first optimum (Opt) and with orthosis mechanisms on but with brake duration of 25ms and delay time of 40% (Bad). The box represents the standard deviation with the mean mark, while the whiskers represent the 95% confidence interval. The 95% confidence intervals for the mean of each task in each sequence were calculated under the assumption of a normally distributed population" was added. Possible difference in tremor power for Drinking, Pouring and Drawing-Spiral.

Nevertheless, we present a controller that provides adjustability with the presented parameter. Future studies could investigate how far the different control parameters of brake duration and delay time affect the perceived comfort of the wearer.

System Dynamics: The control parameter of the brake was optimized regarding tremor suppression efficacy and voluntary movement preservation but also its influence on the system dynamics (O1.1).

Any change in the system dynamics of the wrist is perceived as a disturbance, especially in the frequency range below 2Hz. Therefore a comfortable modulation of the system dynamics for tremor suppression needs to preserve the dynamic behaviour below 2Hz regarding amplitude magnitude as well as phase shift. Our analysis of the system dynamics proved the superior behaviour of a semi-active mechanism over passive mechanisms with increased tremor suppression combined with increased dynamic behaviour preservation below 2Hz, representing voluntary movements and comfort (see Figure 6).

The bode plot of the system dynamics of G(s) indicated the influence of the brake duration and delay time on the wrist impedance. Those parameters influenced the magnitude change at 6Hz, whereas, with an increase of the brake duration, an increase of magnitude was observed. Over the range 5% to 25% delay time values, the resulting tremor suppression was similar, whereas other frequencies decreased the change of magnitude at 6Hz (Figure 7). At 30% delay time, the notch-filter effect was not observed anymore, and the magnitude was increased at 6Hz compared to 5.98Hz and 6.02Hz. As the brake frequency and the signal frequency have an offset at all frequencies around 6Hz, the brake was always activated to a different time within the cycle, amplifying and mitigating the amplitude depending when activated, cancelling each other out in the overall determined amplitude magnitude. It was also observed that with increasing delay time as well with an increase of the brake duration, the phase shift increased. The analysis of the system dynamics showed the behaviour of the system with different control parameters, where the optimal delay time was 5% with the highest magnitude reduction at 6Hz with the lowest phase shift at 2Hz.

Tremor Simulation: To determine the optimum in an applied context, the system needed to be tested with tremorous data, where natural and tremorous frequencies overlapped and tremorous frequencies shifted. Even though the used dataset of Timmer et al. is based on tremor data of an outstretched hand, elements of voluntary movements were detected.

The summary of optima for each tremor dataset in Figure 8 revealed two optima at about 20ms brake duration with 5% delay time as well as at about 20ms brake duration with 30% delay time. It was also observed that the dataset PD04 had a second local minimum at 24ms and 4%. The two optima had the same brake duration, whereas the delay times were 25% apart, corresponding to a quarter of a cycle. For the optima, the brake was activated either in the up-rise or the down-rise, around the peak of velocity. Comparing those two optima regarding tremor and voluntary movement suppression, it was observed that the optima with 30% delay time had less tremor suppression and also less voluntary movement suppression compared to the 5% delay time. The 5% offset was chosen out of those two options as the ratio between tremor suppression and voluntary movement reduction was higher.

No prior study has identified the optimum duration and delay time for a controlled two-state brake. Herrnstadt et al. defined, with an educated guess, their two-state brake to 25ms brake duration and a delay time of 25% (onset after the velocity peak), which correlates with the second optimum found in this work. They reached a tremor suppression of 88% (PSD) with healthy volunteers.

Performance Determination and Comparison: Comparing our controlled two-state brake to passive linear suppression mechanisms (spring-damper) from literature, we were able to prove the superiority of such a semi-active mechanism regarding tremor suppression and voluntary movement preservation.

Passive, linear dampers always have a trait of between tremor suppression and voluntary movement suppression. Adding a spring mostly suppressed more voluntary movements compared to no spring (see Fig. 9 P1(s) vs P2(s)). The controlled two-stage brake reached combinations of tremor and voluntary suppression, which passive mechanisms cannot achieve. However, the downside of such a semi-active system is the added complexity leading to additional weight, such as the additional electrical components, e.g., battery. We estimated the additional weight for a mobile version with a battery capacity of 1.2Ah for one day of use of 18 hours to be less than 200g.

Case et al. also presented a semi-active system, based on a magneto-rheological damper, suppressing in average 96.3% (28.7dB PSD) tremor on a test bench running the same datasets from wrist movements measurements of five ET and five PD patients [32]. On our test bench with our mechanism, using the same dataset, we observed a mean tremor suppression of 66.5% (PSD). With the actively controlled damper of Case et al., they also suppressed 33% of voluntary movements based on PSD, where an offset to the intended trajectory was not taken into account. The voluntary movements had to work against a resistance force of 0.18Nm (4.5N at 38.9mm lever). Our suppression of voluntary movements of 31.1% is not comparable to those determined in the literature as we used a different calculation method. We introduced and used a new method, the trajectory distance, as opposed to the commonly used PSD. Our proposed method is more accurate and more sensitive to changes in voluntary movements as it takes the amplitude change as well as the phase shift of the voluntary movement into account. The PSD calculates the movement power, which is only based on the acceleration amplitude. Calculating here the PSD for voluntary movement on the test bench gave an increase and decrease of voluntary movements between 57.5% and 46.8% for all ten datasets. This variation in voluntary movements can be explained by the low power level, where a small change leads to a high relative difference. We presented a new method to evaluate voluntary movement suppression for simulations and test benches based on the trajectory of voluntary movement and not solely on the PSD, which is centred on acceleration amplitudes. We propose that future simulations use the here presented trajectory-based voluntary movement evaluation as it also accounts for phase shifts. However, this method cannot be applied to human trials as the intended trajectory differs for each executed movement and is unknown. Here we proposed, additionally to the PSD, questionnaires to determine the perceived impact on voluntary movements.

B. Orthosis Evaluation

We presented a textile integrated tremor suppression prototype with the two-state, semi-active mechanism. The proposed concept and mechanism can in future be extended to the wrist radial-ulnar deviation, the pronation-supination or be applied to other joints like the elbow. The textile integration of the orthosis can provide wearability and therewith promote the acceptability of users. However, textiles bear the challenge of effective force transmission to the human, which can be overcome by reinforcing the load path and increasing locally the stiffness of the textile [77]. Therefore, we integrated a thermoplastic sheet for the force transmission, which could be fit individually in future studies to further improve the force transmission.

Mechanisms transmit mechanical loads to the limb's skeletal structure for effective tremor suppression. Transmission of these forces is mediated by soft tissues such as skin, fat, muscle and ligaments [27] as well as the components of the orthosis such as textiles. The compliance of the soft tissue absorbs forces and adds play to the mechanism. Play in the absorption of small movements, such as tremor, decreases the efficacy of the device. For our textile design concept, the transmission of forces to the musculoskeletal system by textiles through the human soft tissue was a limiting efficacy factor. By preloading, the mechanism play was minimized in the system. With this measure, also comfort was positively influenced as play in the system leads to chafing and irritation of the skin. The participant rated the orthosis as comfortable with activated and deactivated brake (5 out of 6) as well as lightweight, unobtrusive and potentially being worn, confirming that our measures for enhanced wearability had a positive effect on the participant (H2).

Future development needs to integrate such semi-active brake system into textiles, for example, with a textile integrated electromagnetic clutch or textile integrated electrostatic clutch. Such textile integration would contribute to improved wearability compared to the current proof-of-concept prototype. For a fully mobile version, the power supply and control unit can be carried decentralized, e.g., in a backpack. We estimate the power supply and control unit to weigh less than 200g (battery capacity of 1.4 Ah covers an 18 hour day).

1) Orthosis Proof-of-Concept Verification Study: The PSD analysis of the gyroscope data, which was attached at the hand, also included angular velocities potentially caused by the elbow, shoulder as well as upper body. Usually, the flexion-extension of the elbow does not align with the flexion-extension of the wrist, why the elbow did not bias the measurement. The other body movements rather add translational velocities than angular, why their influence was also neglectable. Furthermore, the wrist flexion-extension contains the highest tremor power in the case of action tremor compared to the other DOF in the upper limb [78].

Here we present an orthosis that was perceived as comfortable, preserved all voluntary movements and still suppressed tremor by 41.1%, 55.3% and 26.0% for the tasks Drinking, Pouring and Drawing-Spiral (H1). The tremor power peak and the distribution repetition of the task Drawing-Spiral were lower compared to the other tasks as the participant stabilized his hand on the table while drawing. No tremor suppression was observed in the task Spoon-Up. The same, non-suppressing behaviour for the task Spoon-Up was already observed in a previous study using a passive tremor suppression orthosis [23]. In this context, it appears that the executed tasks matters when evaluating tremor suppression. A possible explanation for this could be that different muscles are active for different tasks which leads to a different sensory-motor

feedback loop. Movement power results shown in Fig. 12 are dominated by Pronation-Supination except for spoon-up which shows a different tremor power pattern. It needs to be noted that we assumed a flexion-extension domination in ET based on literature [39] which is only related to postural tremor. Furthermore, the system dynamics for the different tasks change as weight is added by holding a glass or bottle or the wrist is supported by the table. The average tremor suppression efficacy of the unbiased tasks Drinking, Pouring, and Drawing-Spiral was therewith 40.8%, corresponding to 61% and 52% of the efficacy determined by simulation and test bench, respectively. Even though the magnitude of tremor suppression of simulation, test bench and study do not match does not mean that the results are not valid. The tremor suppression relation between the different tasks match and therewith illustrate that the simulation as well as the test bench depict an idealized human system. Furthermore, the comparison between the optimal brake parameter and the chosen bad parameter confirms and validates the method of using simulation and test bench as idealized system to depict the human dynamics. The difference in magnitude can be led back to the increasing compliance from simulation to test bench and to the human case study. The measured tremor suppression efficacy confirms our simulation and test bench results as only the sequence with the optimized parameter suppressed tremor (H3).

The observed tremor suppression could have been influenced by the placebo effect of the wearer. The wearer was aware when the orthosis was active and when not as forces were transmitted, the brake made hearable noises and vibrated. The study sequence with the bad brake control parameter, which can be seen in this context as the control sequence, did not show a change in tremor power, demonstrating that the placebo effect did here not apply. A further potential influence on the tremor suppression was the induced vibration to the forearm by the brake. Such induced vibration is a therapy method in tremor treatment [15]. Displacement amplitude reductions of 28% are reported in tuned and optimized vibration therapies [74]. Here the vibration was not tuned regarding amplitude, location nor did the vibration have the required frequency of 70Hz [79]. The measured tremor suppression can therewith be attributed to the controlled two-state orthosis.

In comparison to our orthosis, Kalaiarasi and Kumar, using a semi-active pneumatic system to suppress tremor, achieved a tremor reduction of 31% of the acceleration amplitude with one ET participant [29]. Fromme et al. presented a Double Viscous Beam device filled with controllable magneto-rheological fluid with which they suppressed 98% (PSD) of tremor but also 85.9% (PSD) of voluntary movements in one user suffering from ET. For another wearable device applying a passive suppression approach [23] a tremor suppression efficacy of 74% to 82% for the tasks Drinking and Drawing-Spiral was reported. However, voluntary movement was also reduced in these tasks by 68% (±35%) and 48% (±27%), respectively.

A systematic literature review by Fromme et al. showed that average tremor suppression efficacy is 63% for tremorous patients, determined for different DOF, with different types of tremor suppression mechanisms and different evaluations methods (e.g., PSD) [37]. Overall, this proof-of-concept study confirms our hypothesis (H1) that the proposed semi-active tremor suppression orthosis suppressed tremor in a similar magnitude to existing systems while preserving more voluntary movements.

Next to our first study with a passive tremor suppression orthosis, we are the first to publish a task differentiation of tremor suppression efficacy in a semi-active orthosis for different activities of daily living.

C. Outlook

We presented an orthosis that suppresses tremor in wrist flexion-extension. This mechanism can be transferred to other DOFs, such as wrist radial-ulnar deviation or even other joints like the elbow and fingers. This study proved the feasibility of such a controlled two-state mechanism, which was here realized with an electromagnetic clutch. In the future, such a mechanism can be implemented into textiles by incorporating conductive components to realize an electromagnetic clutch or textile integrated electrostatic clutch. Conductive laser welding is a method with which robust, conductive, textile integrated surfaces can be realized for such an application [80]. Such textile integration would contribute to higher wearability compared to the current proof-of-concept prototype. Furthermore, a future version of the orthosis could implement an interface with which the user itself can adjust the suppression of voluntary movements by reducing the tremor suppression.

The emphasis of this work was put on tremor suppression by preserving voluntary movements. The connection of the orthosis to the human limb and therewith the efficient transmission of forces through the soft tissue remains a limiting factor in this field. A systematic analysis and investigation for optimal transmission of forces to the human bone structure would improve wearable devices such as the presented one.

Future studies would need to further investigate how far the different control settings of brake duration and delay time affect the perceived comfort of the wearer. An evaluation of a diverse patient group would give insights into the orthosis benefits. Also, a study investigating the progression of tremor while wearing the orthosis regularly for weeks or months could reveal the long term effect of such an orthosis like a temporary reduction of tremor.

The presented controlled, two-state mechanism could also be used to intervene in other movement disorders such as spasticity or the mouthing observed in the Rett syndrome. The mechanism is also suitable for other wearable applications, such as impedance manipulation in wearable robotics or orthoses for metabolic energy saving [81]. Load bearing of the human skeletal system while lifting or adding stability during the stands phase in exosuit supported walking are potential applications.

V. Conclusion

Our semi-active tremor suppression mechanism optimized the trade-off between tremor suppression and voluntary movement suppression. For a two-state, mechanical notch filter

suppression mechanism, two optimal settings for the brake duration, as well as the delay time, exist. The first optimum has higher tremor suppression and voluntary movement suppression, whereas the second has a lower tremor and voluntary movement suppression. Such semi-active tremor suppression preserves more voluntary movements while suppressing more tremor compared to linear passive suppression.

In a proof-of-concept study with one user suffering from ET, the efficacy of the mechanisms implemented into a textile orthosis was verified by differentiating between activities of daily living. The tremor suppression efficacy varied between the tasks Drinking, Pouring, and Drawing-Spiral, whereas in Spoon-Up, no tremor was suppressed. Future studies need to differentiate between those standardized tasks to better depict and optimize the orthosis performance in an applied context.

The three efficacy verification methods, simulation, test bench and human study, have never been put into relation to each other. Here, we present for the first time a decreasing tremor suppression efficacy in the wrist flexion-extension for the computer simulation, test bench and proof-of-concept study of 78.8%, 66.5% and 40.8% (PSD). From past and future simulation and test bench results can now, for the first time, the efficacy on the human roughly be estimated.

Computer simulations are a fast and cost-efficient tool to optimize tremor suppression orthoses. However, test benches are still required to validate the results and used model. The orthosis performance cannot directly be translated to human trials, but we proved that the indicated ratio between tremor suppression and voluntary movements can be.

For the first time, we present a textile integrated, controlled, two-state brake tremor orthosis that suppresses tremor while preserving voluntary movements and having high rated wearability with human trials. Thus this new orthosis, with the presented parameter, has the potential to become a wearable device worn throughout a day, contributing to an improvement of quality of life for tremor affected people.

Such mechanisms can also be used for other involuntary movements or be integrated into other wearable devices where an adaptation of human impedance is advantageous, for example, exosuits.

ACKNOWLEDGMENT

The authors thank the CHT Switzerland AG for providing the silicon and therewith support this work. The authors would also like to express their gratitude to the participant who volunteered in the study.

REFERENCES

[1] G. Deuschl et al., "Consensus statement of the movement disorder society on tremor," *Mov. Disord.*, vol. 13, no. S3, pp. 2–23, 1998, doi: 10.1002/mds.870131303.

[2] R. Elble et al., "Task force report: Scales for screening and evaluating tremor: Critique and recommendations," *Mov. Disord.*, vol. 28, no. 13, pp. 1793–1800, 2013, doi: 10.1002/mds.25648.

[3] R. Elble and G. Deuschl, "Milestones in tremor research," *Mov. Disord.*, vol. 26, no. 6, pp. 1096–1105, 2011, doi: 10.1002/mds.23579.

[4] G. Ellrichmann, "Vorkommen und Wertigkeit von Oberfrequenzen in der 24-Stunden-Elektromyographie und Accelerometrie bei," M.S. thesis, Med. School, Ruhr-Universität Bochum, Bochum, Germany, 2007.

[5] J. Raethjen, M. Lindemann, H. Schmaljohann, R. Wenzelburger, G. Pfister, and G. Deuschl, "Multiple oscillators are causing parkinsonian and essential tremor," *Mov. Disord.*, vol. 15, no. 1, pp. 84–94, 2000, doi: 10.1002/1531-8257(200001)15:1<84::AID-MDS1014>3.0.CO;2-K.

[6] K. Lopez-de-Ipiña et al., "Automatic non-linear analysis of non-invasive writing signals, applied to essential tremor," *J. Appl. Log.*, vol. 16, pp. 50–59, Jul. 2016, doi: 10.1016/j.jal.2015.02.003.

[7] J.-Y. Li et al., "Lewy bodies in grafted neurons in subjects with Parkinson's disease suggest host-to-graft disease propagation," *Nat. Med.*, vol. 14, no. 5, pp. 501–503, 2008, doi: 10.1038/nm1746.

[8] E. D. Louis and J. J. Ferreira, "How common is the most common adult movement disorder? Update on the worldwide prevalence of essential tremor," *Mov. Disord.*, vol. 25, no. 5, pp. 534–541, 2010, doi: 10.1002/mds.22838.

[9] E. D. Louis, L. S. Dure, and S. Pullman, "Essential tremor in childhood: A series of nineteen cases," *Mov. Disord.*, vol. 16, no. 5, pp. 921–923, 2001, doi: 10.1002/mds.1182.

[10] E. D. Louis and R. Ottman, "Study of possible factors associated with age of onset in essential tremor," *Mov. Disord.*, vol. 21, no. 11, pp. 1980–1986, 2006, doi: 10.1002/mds.21102.

[11] K. P. Bhatia et al., "Consensus statement on the classification of tremors. From the task force on tremor of the international parkinson and movement disorder society," *Mov. Disord.*, vol. 33, no. 1, pp. 75–87, 2018, doi: 10.1002/mds.27121.

[12] G. Grimaldi and M. Manto, "'Old' and emerging therapies of human tremor," *Clin. Med. Insights Ther.*, vol. 2, p. CMT.S2999, Mar. 2010, doi: 10.4137/cmt.s2999.

[13] V. Ruonala, A. Meigal, S. M. Rissanen, O. Airaksinen, M. Kankaanpää, and P. A. Karjalainen, "EMG signal morphology and kinematic parameters in essential tremor and Parkinson's disease patients," *J. Electromyogr. Kinesiol.*, vol. 24, no. 2, pp. 300–306, 2014, doi: 10.1016/j.jelekin.2013.12.007.

[14] W. C. Koller, "Pharmacologic treatment of parkinsonian tremor," *Arch. Neurol.*, vol. 43, no. 2, pp. 126–127, 1986, doi: 10.1001/archneur.1986.00520020020009.

[15] R. J. O'Connor and M. U. Kini, "Non-pharmacological and non-surgical interventions for tremor: A systematic review," *Park. Relat. Disord.*, vol. 17, no. 7, pp. 509–515, 2011, doi: 10.1016/j.parkreldis.2010.12.016.

[16] N. L. Diaz and E. D. Louis, "Survey of medication usage patterns among essential tremor patients: Movement disorder specialists vs. general neurologists," *Park. Relat. Disord.*, vol. 16, no. 9, pp. 604–607, 2010, doi: 10.1016/j.parkreldis.2010.07.011.

[17] M. I. Hariz, S. Rehncrona, N. P. Quinn, J. D. Speelman, and C. Wensing, "Multicenter study on deep brain stimulation in Parkinson's disease: An independent assessment of reported adverse events at 4 years," *Mov. Disord.*, vol. 23, no. 3, pp. 416–421, 2008, doi: 10.1002/mds.21888.

[18] S. H. J. Keus, M. Munneke, M. J. Nijkrake, G. Kwakkel, and B. R. Bloem, "Physical therapy in Parkinson's disease: Evolution and future challenges," *Mov. Disord.*, vol. 24, no. 1, pp. 1–14, 2009, doi: 10.1002/mds.22141.

[19] A. Karamesinis, R. V. Sillitoe, and A. Z. Kouzani, "Wearable peripheral electrical stimulation devices for the reduction of essential tremor: A review," *IEEE Access*, vol. 9, pp. 80066–80076, 2021, doi: 10.1109/ACCESS.2021.3084819.

[20] J. Á. Gallego, E. Rocon, J. M. Belda-Lois, and J. L. Pons, "A neuroprosthesis for tremor management through the control of muscle co-contraction," *J. Neuroeng. Rehabil.*, vol. 10, no. 1, p. 36, Apr. 2013, doi: 10.1186/1743-0003-10-36.

[21] A. Pascual-Valdunciel, A. Rajagopal, J. L. Pons, and S. Delp, "Non-invasive electrical stimulation of peripheral nerves for the management of tremor," *J. Neurol. Sci.*, vol. 435, Apr. 2022, Art. no. 120195. [Online]. Available: https://doi.org/10.1016/j.jns.2022.120195

[22] A. Pascual-Valdunciel et al., "Peripheral electrical stimulation to reduce pathological tremor: A review," *J. Neuroeng. Rehabil.*, vol. 18, no. 1, p. 33, 2021, doi: 10.1186/s12984-021-00811-9.

[23] N. P. Fromme, M. Camenzind, R. Riener, and R. M. Rossi, "Design of a lightweight passive orthosis for tremor suppression," *J. Neuroeng. Rehabil.*, vol. 17, no. 1, p. 47, Apr. 2020, doi: 10.1186/s12984-020-00673-7.

[24] E. Rocon, J. Á. Gallego, J. M. Belda-Lois, J. Benito-León, and J. L. Pons, "Biomechanical loading as an alternative treatment for tremor: A review of two approaches," *Tremor Hyperkinetic Mov.*, vol. 2, pp. 1–13, Oct. 2012, doi: 10.5334/TOHM.107.

[25] E. Rocon, J. A. Gallego, J. M. Belda-Lois, and J. L. Pons, *Assistive Robotics as Alternative Treatment for Tremor* (Advances in Intelligent Systems and Computing), vol. 252, A. Sanfeliu, M. Ferre, and M. A. Armada, Eds. Cham, Switzerland: Springer-Verlag, 2014, pp. 173–179, doi: 10.1007/978-3-319-03413-3_12.

[26] J. Kotovsky and M. J. Rosen, "A wearable tremor-suppression orthosis," *J. Rehabil. Res. Dev.*, vol. 35, no. 4, pp. 373–387, 1998.

[27] R. C. V. Loureiro, J. M. Belda-Lois, E. R. Lima, J. L. Pons, J. J. Sanchez-Lacuesta, and W. S. Harwin, "Upper limb tremor suppression in ADL via an orthosis incorporating a controllable double viscous beam actuator," in *Proc. IEEE 9th Int. Conf. Rehabil. Robot.*, 2005, pp. 119–122, doi: 10.1109/ICORR.2005.1501065.

[28] J. Q. Li, X. Z. Zang, and J. Zhao, "Tremor suppression method via magnetorheological damper and fuzzy neural network control," *J. Donghua Univ.*, vol. 27, no. 4, pp. 486–490, 2010.

[29] A. Kalaiarasi and L. A. Kumar, "Sensor based portable tremor suppression device for stroke patients," *Acupuncture Electro-Therapeutics Res.*, vol. 43, no. 1. pp. 29–37, 2018, doi: 10.3727/036012918X15202760634923.

[30] D. Case, B. Taheri, and E. Richer, "Multiphysics modeling of magnetorheological dampers," *Int. J. Multiphys.*, vol. 7, no. 1, pp. 61–76, 2013, doi: 10.1260/1750-9548.7.1.61.

[31] D. Case, B. Taheri, and E. Richer, "Design and characterization of a small-scale magnetorheological damper for tremor suppression," *IEEE/ASME Trans. Mechatronics*, vol. 18, no. 1, pp. 96–103, Feb. 2013, doi: 10.1109/TMECH.2011.2151204.

[32] D. Case, B. Taheri, and E. Richer, "Active control of MR wearable robotic orthosis for pathological tremor suppression," in *Proc. Dyn. Syst. Control Conf.*, vol. 3, 2015, Art. no. V003T42A004, doi: 10.1115/DSCC2015-9874.

[33] D. Case, B. Taheri, and E. Richer, "A lumped-parameter model for adaptive dynamic MR damper control," *IEEE/ASME Trans. Mechatronics*, vol. 20, no. 4, pp. 1689–1696, Aug. 2015, doi: 10.1109/TMECH.2014.2347898.

[34] D. Case, B. Taheri, and E. Richer, "Dynamical modeling and experimental study of a small-scale magnetorheological damper," *IEEE/ASME Trans. Mechatronics*, vol. 19, no. 3, pp. 1015–1024, Jun. 2014, doi: 10.1109/TMECH.2013.2265701.

[35] D. Case, B. Taheri, and E. Richer. "Dynamic magnetorheological damper for orthotic tremor suppression." HUIC Math Engineering. 2011. [Online]. Available: http://huichawaii.org/assets/richer,-edmond-1.pdf

[36] G. Herrnstadt and C. Menon, "On–off tremor suppression orthosis with electromagnetic brake," *Int. J. Mech. Eng. Mechatronics*, vol. 1, no. 2, pp. 7–24, 2013, doi: 10.11159/ijmem.2013.002.

[37] N. P. Fromme, M. Camenzind, R. Riener, and R. M. Rossi, "Need for mechanically and ergonomically enhanced tremor-suppression orthoses for the upper limb: A systematic review," *J. Neuroeng. Rehabil.*, vol. 16, no. 1, pp. 1–15, 2019, doi: 10.1186/s12984-019-0543-7.

[38] M. Xiloyannis et al., "Soft robotic suits: State of the art, core technologies, and open challenges," *IEEE Trans. Robot.*, vol. 38, no. 3, pp. 1343–1362, Jun. 2022, doi: 10.1109/TRO.2021.3084466.

[39] D. W. Geiger, "Characterization of postural tremor in essential tremor using a seven-degree-of-freedom model," M.S. thesis, Dept. Mech. Eng., Ira A. Fulton Coll. Eng. Technol., Tempe, AZ, USA, 2014.

[40] G. Deuschl, J. Raethjen, M. Lindemann, and P. Krack, "The pathophysiology of tremor," *Muscle Nerve*, vol. 24, no. 6, pp. 716–735, Jun. 2001, doi: 10.1002/mus.1063.

[41] V. Sanchez, C. J. Walsh, and R. J. Wood, "Textile technology for soft robotic and autonomous garments," *Adv. Func. Mater.*, vol. 31, no. 6, Feb. 2021, Art. no. 2008278, doi: 10.1002/adfm.202008278.

[42] C. J. Nycz, M. A. Delph, and G. S. Fischer, "Modeling and design of a tendon actuated soft robotic exoskeleton for hemiparetic upper limb rehabilitation," in *Proc. Annu. Int. Conf. IEEE Eng. Med. Biol. Soc. (EMBS)*, Nov. 2015, pp. 3889–3892, doi: 10.1109/EMBC.2015.7319243.

[43] D. Asane, A. Schmitz, and S. Sugano, "Investigating the strain behaviour of Dyneema under cyclic loads," in *Proc. JSME Annu. Conf. Robot. Mechatronics*, 2020, p. 1P2-K05, doi: 10.1299/jsmermd.2020.1p2-k05.

[44] M. van der Stelt et al., "Improving lives in three dimensions: The feasibility of 3D printing for creating personalized medical aids in a rural area of Sierra Leone," *Am. J. Trop. Med. Hyg.*, vol. 102, no. 4, pp. 905–909, Apr. 2020, doi: 10.4269/ajtmh.19-0359.

[45] *Active Clutch Line*, Kendrion, Villingen-Schwenningen, Germany, 2019.

[46] E. Rocon, J. M. Belda-Lois, A. F. Ruiz, M. Manto, J. C. Moreno, and J. L. Pons, "Design and validation of a rehabilitation robotic exoskeleton for tremor assessment and suppression," *IEEE Trans. Neural Syst. Rehabil. Eng.*, vol. 15, pp. 367–378, 2007, doi: 10.1109/TNSRE.2007.903917.

[47] B. Taheri, "Real-time pathological tremor identification and suppression in human arm via active orthotic devices," Ph.D. dissertation, Dept. Mech. Eng., Southern Methodist Univ., Dallas, TX, USA, 2005.

[48] C. N. Riviere, *Adaptive Suppression of Tremor for Improved Human–Machine Control*, UMI, Ann Arbor, MI, USA, 1995.

[49] K. C. Veluvolu, W. T. Latt, and W. T. Ang, "Double adaptive bandlimited multiple Fourier linear combiner for real-time estimation/filtering of physiological tremor," *Biomed. Signal Process. Control*, vol. 5, no. 1, pp. 37–44, 2010, doi: 10.1016/j.bspc.2009.06.001.

[50] Y. Zhou, M. E. Jenkins, M. D. Naish, and A. L. Trejos, "Development of a wearable tremor suppression glove," in *Proc. IEEE RAS EMBS Int. Conf. Biomed. Robot. Biomechatronics*, Aug. 2018, pp. 640–645, doi: 10.1109/BIOROB.2018.8487197.

[51] J. A. Gallego, E. Rocon, J. O. Roa, J. C. Moreno, and J. L. Pons, "Real-time estimation of pathological tremor parameters from gyroscope data," *Sensors*, vol. 10, no. 3, pp. 2129–2149, 2010, doi: 10.3390/s100302129.

[52] C. Mazzà, M. Donati, J. McCamley, P. Picerno, and A. Cappozzo, "An optimized Kalman filter for the estimate of trunk orientation from inertial sensors data during treadmill walking," *Gait Posture*, vol. 35, no. 1, pp. 138–142, 2012, doi: 10.1016/j.gaitpost.2011.08.024.

[53] R. E. Kalman, "A new approach to linear filtering and prediction problems," *J. Fluids Eng. Trans. ASME*, vol. 82, no. 1, pp. 35–45, 1960, doi: 10.1115/1.3662552.

[54] G. Welch and G. Bishop, "An introduction to the Kalman filter," Dept. Comput. Sci., Univ. North Carolina, Chapel Hill, NC, USA, Rep. TR 95-041, 2006. [Online]. Available: https://www.cs.unc.edu/∼welch/media/pdf/kalman_intro.pdf

[55] S. M. Hashemi, M. F. Golnaraghi, and A. E. Patla, "Tuned vibration absorber for suppression of rest tremor in Parkinson's disease," *Med. Biol. Eng. Comput.*, vol. 42, no. 1, pp. 61–70, 2004, doi: 10.1007/BF02351012.

[56] B. Taheri, D. Case, and E. Richer, "Adaptive suppression of severe pathological tremor by torque estimation method," *IEEE/ASME Trans. Mechatronics*, vol. 20, no. 2, pp. 717–727, Apr. 2015, doi: 10.1109/TMECH.2014.2317948.

[57] G. Herrnstadt and C. Menon, "Elbow orthosis for tremor suppression—A torque based input case," in *Bioinformatics and Biomedical Engineering* (Lecture Notes in Computer Science, 10208 (Lecture Notes in Artificial Intelligence and Lecture Notes in Bioinformatics)). Cham, Switzerland: Springer, 2017, pp. 292–302, doi: 10.1007/978-3-319-56148-6_25.

[58] E. Rocon, M. Manto, J. Pons, S. Camut, and J. M. Belda, "Mechanical suppression of essential tremor," *Cerebellum*, vol. 6, no. 1, pp. 73–78, 2007, doi: 10.1080/14734220601103037.

[59] D. C. Lin and W. Z. Rymer, "Damping actions of the neuromuscular system with inertial loads: Soleus muscle of the decerebrate cat," *J. Neurophysiol.*, vol. 83, no. 2, pp. 652–658, 2000, doi: 10.1152/jn.2000.83.2.652.

[60] B. Taheri, D. Case, and E. Richer, "Robust controller for tremor suppression at musculoskeletal level in human wrist," *IEEE Trans. Neural Syst. Rehabil. Eng.*, vol. 22, pp. 379–388, 2014, doi: 10.1109/TNSRE.2013.2295034.

[61] B. Taheri, D. Case, and E. Richer, "Active tremor estimation and suppression in human elbow joint," in *Proc. ASME Dyn. Syst. Control Conf. Bath/ASME Symp. Fluid Power Motion Control (DSCC)*, vol. 2, 2011, pp. 115–120, doi: 10.1115/DSCC2011-6185.

[62] B. Taheri, D. Case, and E. Richer, "Theoretical development and experimental validation of an adaptive controller for tremor suppression at musculoskeletal level," in *Proc. ASME Dyn. Syst. Control Conf. (DSCC)*, vol. 2, 2013, pp. 1–8, doi: 10.1115/DSCC2013-3954.

[63] G. Herrnstadt and C. Menon, "Voluntary-driven elbow orthosis with speed-controlled tremor suppression," *Front. Bioeng. Biotechnol.*, vol. 4, pp. 1–10, Mar. 2016, doi: 10.3389/fbioe.2016.00029.

[64] G. Herrnstadt and C. Menon, "Admittance-based voluntary-driven motion with speed-controlled tremor rejection," *IEEE/ASME Trans. Mechatronics*, vol. 21, no. 4, pp. 2108–2119, Aug. 2016, doi: 10.1109/TMECH.2016.2555811.

[65] A. H. Zamanian and E. Richer, "Adaptive disturbance rejection controller for pathological tremor suppression with permanent magnet linear motor," in *Proc. ASME Dyn. Syst. Control Conf.*, vol. 1, 2017, Art. no. V001T37A003, doi: 10.1115/DSCC2017-5151.

[66] M. Takanokura, R. Sugahara, N. Miyake, K. Ishiguro, T. Muto, and K. Sakamoto, "Upper-limb orthoses implemented with air dashpots for suppression of pathological tremor in daily activites," in *Proc. ISB Conf.*, Jul. 2011, pp. 3–4.

[67] T. D. C. Busarello and M. G. Simões, "A tutorial on implementing Kalman filters with commonly used blocks," in *Proc. IECON 45th Annu. Conf. IEEE Ind. Electron. Soc.*, Oct. 2019, pp. 60–67, doi: 10.1109/IECON.2019.8927549.

[68] J. Timmer, S. Häussler, M. Lauk, and C. H. Lücking, "Pathological tremors: Deterministic chaos or nonlinear stochastic oscillators?" *Chaos*, vol. 10, no. 1, pp. 278–288, 2000, doi: 10.1063/1.166494.

[69] P. D. Welch, "The use of fast Fourier transform for the estimation of power spectra: A method based on time averaging over short, modified periodograms," *IEEE Trans. Audio Electroacoust.*, vol. AE-15, no. 2, pp. 70–73, Jun. 1967, doi: 10.1109/TAU.1967.1161901.

[70] G. Grimaldi and M. Manto, *Mechanisms and Emerging Therapies in Tremor Disorders*. New York, NY, USA: Springer, 2013, doi: 10.1007/978-1-4614-4027-7.

[71] C. J. Needham and R. D. Boyle, "Performance evaluation metrics and statistics for positional tracker evaluation," in *Proc. Int. Conf. Comput. Vis. Syst.*, 2003, pp. 278–289.

[72] D. A. Heldman, J. Jankovic, D. E. Vaillancourt, J. Prodoehl, R. J. Elble, and J. P. Giuffrida, "Essential tremor quantification during activities of daily living," *Park. Relat. Disord.*, vol. 17, no. 7, pp. 537–542, 2011, doi: 10.1016/j.parkreldis.2011.04.017.

[73] R. Katz, E. Buki, and M. Zacksenhouse, "Attenuating tremor using passive devices," *Stud. Health Technol. Inform.*, vol. 242, pp. 741–747, Jan. 2017, doi: 10.3233/978-1-61499-798-6-741.

[74] A. L. Pando, H. Lee, W. B. Drake, N. Hogan, and S. K. Charles, "Position-dependent characterization of passive wrist stiffness," *IEEE Trans. Biomed. Eng.*, vol. 61, no. 8, pp. 2235–2244, Aug. 2014, doi: 10.1109/TBME.2014.2313532.

[75] S. K. Charles and N. Hogan, "Dynamics of wrist rotations," *J. Biomech.*, vol. 44, no. 4, pp. 614–621, Feb. 2011, doi: 10.1016/j.jbiomech.2010.11.016.

[76] S. Pledgie, K. E. Barner, S. K. Agrawal, and T. Rahman, "Tremor suppression through impedance control," *IEEE Trans. Rehabil. Eng.*, vol. 8, no. 1, pp. 53–59, Mar. 2000.

[77] D. Chiaradia, M. Xiloyannis, C. W. Antuvan, A. Frisoli, and L. Masia, "Design and embedded control of a soft elbow exosuit," in *Proc. IEEE Int. Conf. Soft Robot. (RoboSoft)*, 2018, pp. 565–571, doi: 10.1109/ROBOSOFT.2018.8405386.

[78] D. W. Geiger, D. L. Eggett, and S. K. Charles, "A method for characterizing essential tremor from the shoulder to the wrist," *Clin. Biomech.*, vol. 52, pp. 117–123, Feb. 2018, doi: 10.1016/j.clinbiomech.2017.12.003.

[79] P. Feys et al., "Online movement control in multiple sclerosis patients with tremor: Effects of tendon vibration," *Mov. Disord.*, vol. 21, no. 8, pp. 1148–1153, 2006, doi: 10.1002/mds.20938.

[80] N. P. Fromme, Y. Li, M. Camenzind, C. Toncelli, and R. M. Rossi, "Metal-textile laser welding for wearable sensors applications," *Adv. Electron. Mater.*, vol. 7, no. 4, pp. 1–9, 2021, doi: 10.1002/aelm.202001238.

[81] E. Etenzi, R. Borzuola, and A. M. Grabowski, "Passive-elastic knee-ankle exoskeleton reduces the metabolic cost of walking," *J. Neuroeng. Rehabil.*, vol. 17, no. 1, p. 104, Dec. 2020, doi: 10.1186/s12984-020-00719-w.